Where and When Does Streamflow Regulation Significantly Affect Climate Change Outcomes in the Columbia River Basin?

Jane Harrell

A thesis

submitted in partial fulfillment of the

requirements for the degree of

Master of Science in Civil Engineering

University of Washington

2021

Committee:

Bart Nijssen

Erkan Istanbulluoglu

Chris Frans

Jeffrey Arnold

Program Authorized to Offer Degree:

Civil and Environmental Engineering

University of Washington

Abstract

Where and When Does Streamflow Regulation Significantly Affect Climate Change Outcomes in the Columbia River Basin?

Jane Harrell

Chair of the Supervisory Committee:

Professor Bart Nijssen

Civil and Environmental Engineering

The Columbia River basin is a large transboundary basin located in the Pacific Northwest, straddling the US-Canadian border. The basin spans seven US states and one Canadian province, encompassing a diverse range of hydroclimates. Strong seasonality and complex topography, combined with the prominent role of snow in the hydrologic cycle, give rise to spatially heterogeneous climate impacts on unregulated streamflow. The basin's water resources are economically critical for the region, and regulation across the domain is extensive. This study investigates where and when regulation significantly affects projected changes in streamflow due to climate change by comparing climate outcomes across 80-member ensembles of unregulated and regulated streamflow projections at 75 sites across the Columbia River basin. Unregulated daily streamflow projections are taken from an existing dataset of climate projections. Regulated

streamflow projections were modeled by the US Army Corps of Engineers and the US Bureau of Reclamation by hydro-regulation models that simulate system operations based on current and historical water demands. Regulation dampens large shifts in winter and summer streamflow volumes and cool-season high flow extremes. Results for changes in warm-season high flow extremes and dry-season low flow extremes are spatially variable. At historically snow dominant headwater reservoirs, regulation amplifies the change in warm-season high-flow extremes, but these effects generally diminish downstream where, in some cases, dampening effects occur. Regulation dampens dry-season low flow changes in headwater tributaries where regulation is large, but elsewhere regulation has little effect on changes in dry-season low flows.

Table of Contents

List of Figures

Acknowledgements

I would like to thank my advisor Bart Nijssen for not only supporting and offering mentorship throughout my master's thesis research but for supporting my undergraduate research. Bart's guidance has played a fundamental role in the development of my academic foundation and research career in hydrology. I also thank the "climate team" and others at the US Army Corps of Engineers, Chris Frans, Jason Chang, Keith Duffy, Jeremy Giovando, Evan Heisman, Kristian Mickelson, Reyn Aoki, Jeff Arnold, and John England, for their shared wisdom and expertise in water resources management and hydrologic analysis. To all of the folks with the UW Hydro | Computational Hydrology group, I appreciate your support and mentorship throughout this journey.

The regulated and unregulated streamflow datasets used in this study were developed through a collaboration between the US Army Corps of Engineers, the Bureau of Reclamation, the Bonneville Power Administration, Oriana Chegwidden and Bart Nijssen with the University of Washington, and David Rupp with Oregon State University. I appreciate all collaborators who developed the datasets to make this work possible.

This material is based upon work supported by the National Science Foundation Graduate Research Fellowship under Grant No. DGE-1762114.

1. Introduction

The Columbia River basin is responsible for 77% of coastal drainage in the Northwestern US (Barnes et al., 1972) and is the sixth largest basin by drainage area in the United States (Kammerer, 1990). Located in the Pacific Northwest, the basin spans seven states and straddles the US-Canadian border, encompassing a diverse range of hydroclimates and topography. The 4th National Climate Assessment states that 21st century temperatures are projected to rise for all greenhouse gas emission scenarios and extreme precipitation events are increasing (Reidmiller et al., 2018). The natural hydrology of the Pacific Northwest is particularly sensitive to shifts in climate due to the region's complex topography, the prominent role of snow in warm-season streamflow, and strong seasonality of the annual hydrograph (Elsner et al., 2010; Vano, 2015).

Across the domain, diverse hydroclimate and topography are projected to lead to spatiotemporally heterogeneous climate impacts. Over the past century, the Pacific Northwest has warmed by nearly 1ºC, and temperatures are projected to continue to rise (May et al., 2018). At upper elevations, warming temperatures have already resulted in declines in glacial extent (Frans et al., 2018; Moore et al., 2020) and are projected to lead to significant depletions in seasonal snowpack (Elsner et al., 2010; Gergel et al., 2017; Lute et al., 2015; RMJOC-II, 2018). At lower elevations, more cool-season precipitation will likely fall as rain rather than snow (Musselman et al., 2018; Salathé et al., 2018). Mountain snowpack serves as a natural reservoir of fresh water and diminishing snowpack could lead to more frequent and severe drought events (Chegwidden et al., 2019; Leppi et al., 2012; RMJOC-II, 2018; Tohver et al., 2014). Tohver et al. (2014) found that low flow extremes will be more prominent in wetter regions of the Pacific Northwest, where warm-season evaporation is historically energy-limited rather than water-

limited. Seasonal precipitation patterns are also projected to amplify under climate change. Precipitation is projected to increase in the autumn, winter, and spring, and decrease in the summer during the dry season (RMJOC-II, 2018; Rupp et al., 2016; Tohver et al., 2014). The largest seasonal increases are likely to occur in winter, which historically is the season with the largest total precipitation. Streamflow timing is seasonally dependent. Changes in annual precipitation patterns and depletions in snowpack will shift peak streamflow timing earlier in the water year for snow dominant and transient rain-snow watersheds (Chegwidden et al., 2019; Fritze et al., 2011; Hamlet et al., 2010; Payne et al., 2004; Stewart et al., 2005). Peak timing shifts will likely be more pronounced in transient watersheds where winter temperatures are at or near freezing levels and therefore more sensitive to warming (Bureau of Reclamation, 2016; Vano et al., 2015). Extreme precipitation events are increasing (IPCC, 2014; May et al., 2018; Warner et al., 2017), and are projected to lead to substantially more severe flood events (Salathé et al., 2014). Queen et al. (2021) projected pervasive increases in Columbia River basin flood magnitudes based on unregulated streamflow projections.

Over the past century, water resource infrastructure has changed the streamflow regime by creating artificial reservoirs and altering flows. While climate is a primary driver of natural basin hydrology, extensive regulation modulates this natural hydrology and thus streamflow (Figure 1). The Columbia River basin is heavily regulated by federal and private agencies for a range of system objectives including flood risk management, hydropower, irrigation, navigation, fish passage, and recreation. More than 250 large reservoirs exist across the system and streamflow regulation sustains an economically critical food-water-energy nexus. Each reservoir has multiple and unique operational constraints that can vary over a given water year depending on local-scale hydroclimate and local and system-wide objectives. Columbia River System

operations follow transnational guidelines defined by the Columbia River Treaty, an international agreement between the US and Canada on how water is allocated across the US-Canadian border. Ratified in 1964, the treaty informs the joint management of three upper Columbia Canadian storage dams to coordinate transboundary flood control and is currently being renegotiated for modernization post-2024 (Stern, 2020).

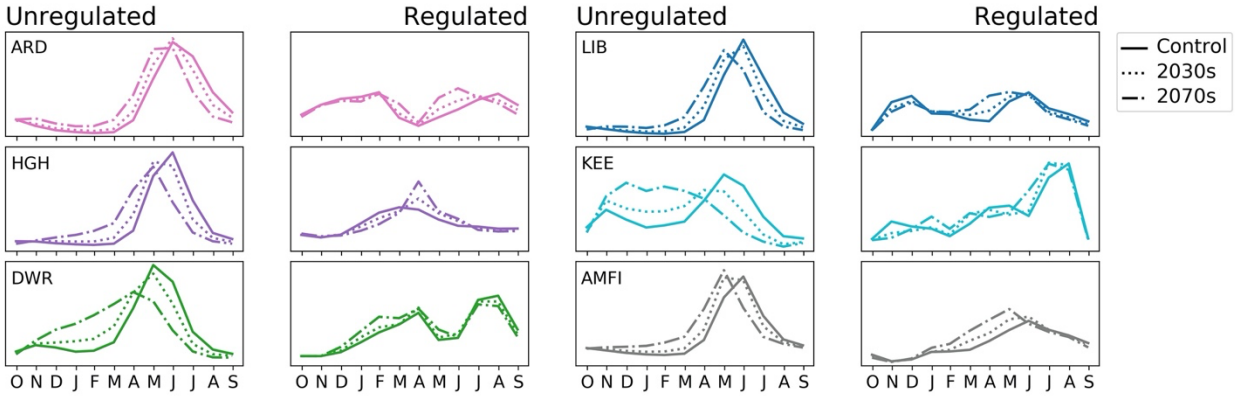

Figure 1. Annual hydrographs of monthly average streamflow for Arrow Lakes (ARD), Libby (LIB), Hungry Horse (HGH), Keechelus (KEE), Dworshak (DWR), and American Falls (AMFI) and the three periods examined: the control period (1976-2005), 2030s (2020-2049), and 2070s (2060-2089). Monthly averages are taken from the median of the ensemble. For each location, the left panel shows the unregulated hydrograph, and the right panel shows the regulated hydrograph.

Many sensitivity studies have investigated climate change impacts on naturalized or unregulated streamflow in the Columbia River basin; however, only a limited number of large-scale studies have considered the large role of regulation. For clarity, we will refer to naturalized streamflow as unregulated streamflow in the remainder of this narrative. To test the reliability and vulnerability of Columbia River system operations under changing historical conditions, Jones and Hammond (2020) investigated observed intra-annual timing of reservoir inflows and outflows. Between 1950 and 2012, May through October inflows declined but outflows increased due to low flow augmentation. These differences were more prominent in 1950 but decreased by 2012. Zhou et al. (2018) investigated the effect of regulation on the timing of

hydrologic regime shifts for large basins across the western US. Their study used statistically downscaled climate projections from three Coupled Model Intercomparison Project version 5 (CMIP5) global climate models (GCMs) for Representative Concentration Pathway (RCP) 4.5 and 8.5 emissions scenarios. GCM meteorology was downscaled to the 1/8-degree grid resolution. Regulated flows were simulated by the Model for Scale Adaptive River Transport (Li et al., 2013) Water Management (Voisin et al., 2013a) model (MOSART-WM); a simplified hydro-regulation model that uses operational rules based on historical monthly mean inflows and water demands. Zhou et al. (2018) found that for the Columbia River basin, regulation delayed the timing of regime shifts for all seasons except autumn and they speculated that effects for winter were the result of seasonally variable water demands. In winter months, reservoirs are emptied in preparation for the spring freshet. Under climate change, unregulated flows are projected to increase during winter while the spring freshet is projected to decrease resulting in more reservoir storage available to mitigate winter changes (Zhou et al., 2018). Studies in subbasins west of the Cascade Mountain range have also shown large differences between projected changes in unregulated and regulated streamflow extremes. In some cases, regulation amplifies the climate signal (Lee et al., 2016, 2018).

To investigate where and when extensive regulation modifies climate impacts on Columbia River basin streamflow, this study uses two 80-member ensembles of unregulated and regulated streamflow projections developed from 10 CMIP5 GCM projections for the RCP 8.5 emissions scenario (RMJOC-II, 2018; RMJOC-II, 2020) to compare climate outcomes under unregulated and regulated conditions. Regulated flow projections were modeled by the US Army Corps of Engineers (USACE) and the US Bureau of Reclamation (USBR) using high resolution hydro-regulation models that are used by USACE and USBR to support long- and short-term

federal water management planning. These models use operational rule-curves based on current and historical water management objectives that vary temporally and spatially and account for local and system-wide flood risk management, hydropower, irrigation, navigation, and ecological constraints (RMJOC-II, 2020). Operational rule-curves are based on current and historical water demands and do not change to account for future changing conditions.

This study seeks to answer two key questions: 1) How does regulation modify projections of streamflow volumes and extreme streamflow events under climate change? 2) How do these results vary seasonally and across the domain? We address these questions by comparing projected climate impacts on seasonal volumes and high and low flow extremes for unregulated conditions and regulated conditions. We investigate changes in extremes for 75 sites across the basin where hydro-regulation was modeled at a daily time step. Seasonal volume changes are examined for 53 sites using output from hydro-regulation models at both a daily and monthly time step. Outcomes for the 2030s (2020-2049) and the 2070s (2060-2089) are compared to the control period (1976-2005), and we test relationships to river network location and the level of regulation by grouping locations by region and the degree of upstream regulation, respectively. The control period is selected to represent the most recent 30-year period in the historical streamflow used to validate simulated flows (RMJOC-II, 2018). The 2030s and 2070s are selected to represent the near future and far future, respectively. Analysis is performed for water years rather than calendar years. A water year is a 12-month period used by hydrologists to represent temporal precipitation patterns that influence the water cycle (e.g., wet-season winter snow accumulation and dry-season summer snow melt) and is defined as October 1 of the previous calendar year through September 30 of the given year.

In the face of climate change, water managers and stakeholders need to determine how to invest in management adaptation strategies that protect the basin's valuable water resources. Identification of the spatial and temporal conditions for which regulation ameliorates or exacerbates climate impacts could help water managers make informed decisions on where and how to allocate water for climate change mitigation and adaptation.

2. Methods

2.1 Study Area

The Columbia River basin is a transnational river system covering 673 thousand km^2 of the Pacific Northwest. The basin encompasses a diverse range of hydroclimates from arid lowlands to glaciated mountain regions. The Cascade and Rocky Mountain ranges pass through the western and eastern edges of the basin, respectively, and high elevation snowpack supplies much of the basin's freshwater through the spring freshet. Three hydrologic regimes exist across the domain (Hamlet and Lettenmaier, 2007): the rain-dominant regime where streamflow peaks in the cool-season primarily driven by rainfall; the transient regime where two annual peak streamflow pulses result from cool-season rainfall and warm-season snowmelt; and the snow-dominant regime where streamflow peaks in the warm-season primarily driven by snowmelt (Elsner et al., 2010). These three regimes can be distinguished by the ratio of peak snow water equivalent (SWE) to cool-season precipitation (Barnet et al, 2005). Pacific Northwest peak SWE typically occurs around April 1. Following the work of Mantua et al. (2010), we classify hydrologic regimes for each 30-year period by the ratio of April 1 SWE to October through March precipitation (SWE/P) where SWE/P less than 0.1 indicates a rain-dominant regime,

SWE/P between 0.1 and 0.4 indicates a transient regime, and SWE/P greater than 0.4 indicates snow-dominant regime (Figure 2).

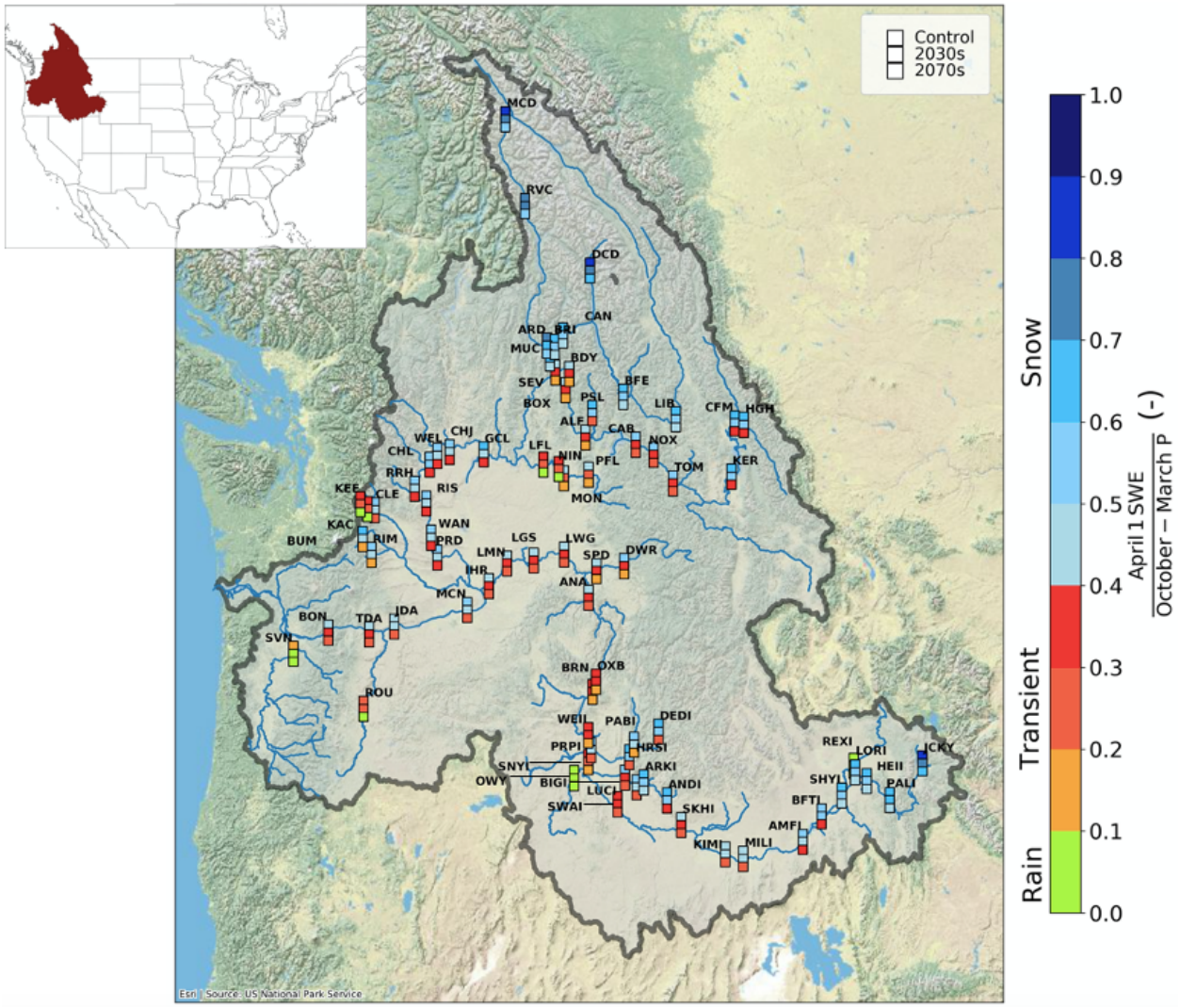

Figure 2. Map of the Columbia River basin and hydrologic regime ratios for the 75 sites and three periods investigated in this study. The basin is located in the Pacific Northwest region of the US straddling the US-Canadian border. Regime classification color scheme adapted from Mantua et al. (2010). Base map provided by Esri (2009).

2.2 Location Groupings

2.2.1 Regions

Hydroclimate across the domain is diverse, and system operations vary widely depending on regional water demands. To test the relationship between regulation effects and river network

location, sites are grouped into ten regions defined by location on a tributary or the mainstem (Figure 3a).

2.2.2 Degree of Upstream Regulation

Regulation effects on unregulated flow can be attributed to temporal reservoir storage and delayed releases that alter streamflow timing (Grill et al., 2019). The degree of upstream regulation (DOR) is a measure of annual storage effects on unregulated streamflow and is defined as total upstream storage capacity normalized by annual streamflow volume (Grill et al., 2019; Lehner et al., 2011; Dynesius and Nillson, 1994). Higher DOR indicates greater capacity to store water throughout the water year and as a result, larger regulation effects on the unregulated flow regime. We group locations by their DOR to test the relationship between annual storage effects and regulated climate outcomes (Figure 3b), with DOR calculated as

$$\mathrm{DOR_j} = \frac{\sum_{i=1}^{n} \mathrm{SV_i}}{\mathrm{AV_j}}, \quad (1)$$

where $\mathrm{DOR_j}$ is the DOR at site j, $\mathrm{SV_i}$ is the storage volume of any reservoir upstream of site j, n is the total number of reservoirs upstream of site j and $\mathrm{AV_j}$ is the unregulated annual streamflow volume at site j (Lehner et al., 2019). To group sites with similar DOR, we applied Eq. 1 during the control period.

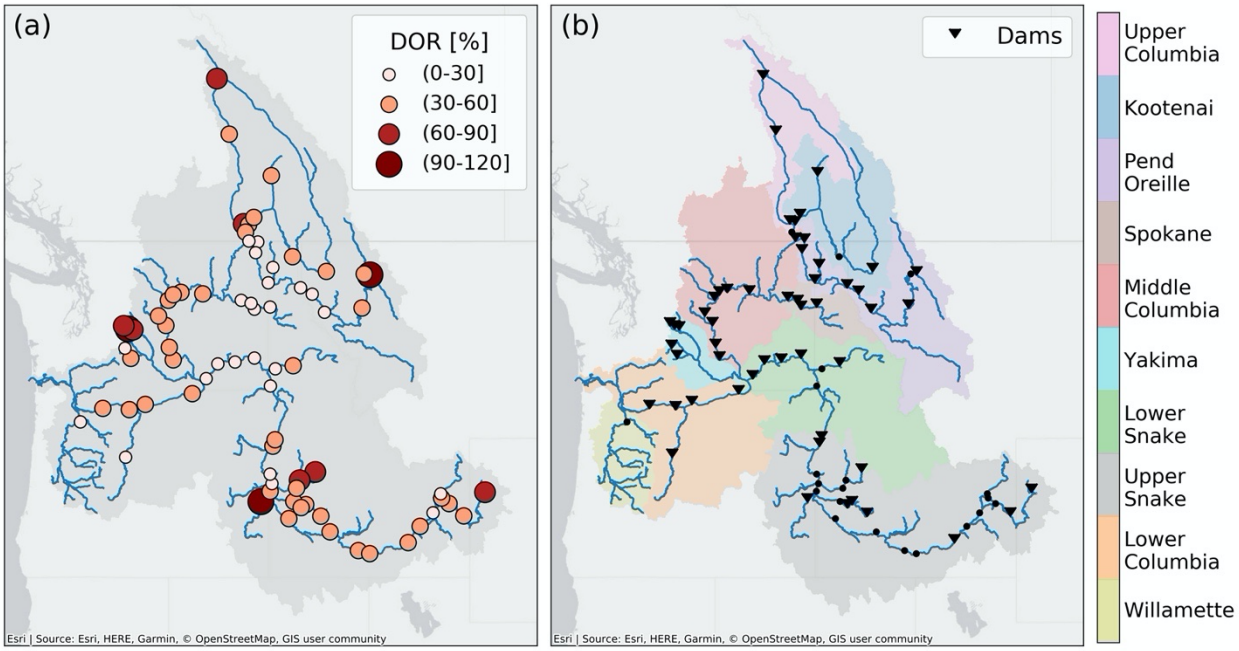

Figure 3. Maps of the spatial groupings used in this study: the degree of upstream regulation (DOR) (a) and region (b). Base map provided by Esri (2011).

2.3 Metrics

2.3.1 Seasonal Volumes

Water demands vary widely across seasons and operational constraints are highly seasonally dependent. As a result, changes in seasonal volumes have been identified by stakeholders as indicators of system vulnerability for a wide range of water management objectives (RMJOC-II, 2020). The hydro-regulation models used to generate the regulated flow ensemble examined in this study use rule-curves that vary by season based on historical hydroclimate; however, the seasonality of unregulated hydrograph is projected to shift under climate change (Figure 1) and large shifts in seasonal volumes may drive large regulation affects. We compare climate change impacts on seasonal volumes by examining the ratio of future seasonal volumes to control period volumes under both unregulated conditions and regulated

conditions for September, October, November (SON); December, January, February (DJF); March, April, May (MAM); and June, July, August (JJA).

2.3.2 Level of Seasonal Volume Regulation

The level of seasonal volume regulation (LR_{sv}) is defined as the ratio of regulated seasonal volume to unregulated seasonal volume,

$$\mathrm{LR_{sv}} = \frac{\text{Regulated Seasonal Volume}}{\text{Unregulated Seasonal Volume}}. \quad (2)$$

LR_{sv} greater than 1 indicates that the regulated seasonal volume exceeds the unregulated seasonal volume while LR_{sv} less than 1 indicates that the regulated seasonal volume is less than the unregulated seasonal volume. We compare control period LR_{sv} to future LR_{sv} to examine how regulation of unregulated volumes is changing in the future. For example, if LR_{sv} is 0.5 during the control period and 0.9 by the 2070s the system is regulating less of the unregulated volume in the future. However, it is important to keep in mind that both the numerator and denominator change when applying Eq. 2 to different periods.

2.3.3 Extremes

Due to extensive flood risk management practices and competing demands for water (e.g., irrigation, municipal water supply, hydropower generation, and ecosystem function), analysis of changes in extremes can provide critical information for adaptation planning. We investigate regulation effects on high flow extremes by comparing 50-year return period peak flow (Q50RP) changes under regulated conditions to unregulated conditions. The Log-Pearson 3 (LP3) distribution curve is fit to regulated and unregulated annual maximum flow time series for each 30-year period. By using a 30-year sample size rather than a larger (e.g., 50 or 75-year) sample size, we limit the effects of non-stationarity in sample statistics used to generate the LP3

curve. We examine 50-year return period (2% annual exceedance probability) maxima rather than 100-year return period maxima due to lower confidence in the 1% annual exceedance probability that results from using a 30-year sample size. From the LP3 distributions, 50-year return period peak flow changes are investigated by calculating the ratio of future to control period Q50RP. The LP3 fit for unregulated high flow extremes is recommended by United States Geological Survey (USGS) Bulletin 17C (England et al., 2018) which established federal guidelines for flood frequency analysis. Regulated high flow frequency curves are typically generated using graphical fitting methods described by Beard and Fredrich (1975); however, we use the LP3 distribution to fit both unregulated and regulated high flow frequency curves in order to apply a consistent framework across a large number of sites. Warming temperatures will shift streamflow maxima towards winter where they historically occurred in spring (indicated by widespread regime shifts across the domain as shown in Figure 2), and seasonally varying operations could explain large changes in regulated Q50RP. To identify seasonal climatic changes and operations that drive annual Q50RP changes, we also examine changes in cool-season (October-March) Q50RP and warm-season (April-September) Q50RP.

We investigate regulation effects on low flow extremes similarly, by comparing 10-year return period 7-day minimum (7Q10) changes under regulated conditions to unregulated conditions. The LP3 distribution curve is fit to regulated and unregulated 7-day minimum flow time series for each 30-year period. From the LP3 distributions, we examine changes in the 10-year return period 7-day minimum by calculating the ratio of future to control period 7Q10. High snow dominance can lead to annual minimums occurring during cool-season snowpack accumulation (Tohver et al. 2014; see Figure 1). Shifts in dry-season low flow extremes can indicate ecosystem vulnerability and motivate changes in late summer and early autumn

ecological operations. Rather than taking the 7Q10 from the annual time series, we limit our analysis to the dry-season (July-October) which encompasses the period of low flow operational constraints across the domain (RMJOC-II, 2020).

2.3.4 Level of Q50RP Regulation

Similar to the level of seasonal volume regulation defined in section 2.3.2, we define the level of Q50RP regulation (LR_{Q50RP}) as the ratio of regulated Q50RP to unregulated Q50RP,

$$LR_{Q50RP} = \frac{\text{Regulated Q50RP}}{\text{Unregulated Q50RP}}. \quad (3)$$

LR_{Q50RP} greater than 1 indicates that the regulated Q50RP exceeds the unregulated Q50RP while LR_{Q50RP} less than 1 indicates the regulated Q50RP is less than the unregulated Q50RP. Because the Q50RP amounts are determined independently from the regulated and unregulated flow time series, they do not necessarily denote the same event. For example, they could occur during different seasons.

3. Data

3.1 Unregulated Streamflow Projections

Unregulated streamflow projections are taken from Chegwidden et al. (2017). This dataset consists of Columbia River basin simulated streamflow at a daily time step from the Precipitation Runoff Modeling System (PRMS; Leavesly et al., 1983) and Variable Infiltration Capacity model (VIC; Liang et al., 1994). Both PRMS and VIC were forced using statistically downscaled CMIP5 GCM projections for the RCP 4.5 and RCP 8.5 emissions scenario. For the purposes of this study, we limit our analysis to emissions scenario RCP 8.5 which is considered the business-as-usual scenario (i.e., the amount of radiative forcing that is projected to occur if

no effort is made to decrease greenhouse gas emissions). GCM forcings were statistically downscaled and bias corrected at the 1/16th degree grid resolution using two different methods: the multivariate adaptive constructed analogs (MACA) method implemented at a daily time step, and the bias correction, spatial disaggregation (BCSD; Wood et al., 2004) downscaling method implemented at a monthly time step. Ten GCMs, two meteorological downscaling methods, two hydrology models, and three model parameter sets for the VIC model resulted in an 80-member ensemble of unregulated streamflow projections for RCP 8.5 at locations across the Pacific Northwest (Chegwidden et al., 2019). From this dataset, we analyze streamflow changes at 75 Columbia River basin locations that map to sites where hydro-regulation was modeled by USACE and USBR.

3.2 Regulated Streamflow Projections

Regulated streamflow projections were developed by USACE and USBR. With the exception of the Yakima, Upper Snake, and Deschutes, regulation across the basin was simulated at a daily-step using the Hydrologic Engineer Center's Reservoir System Simulations model (HEC-ResSim) (USACE, 2013) developed by USACE for Columbia River basin planning studies (RMJOC-II, 2020). This model was recently updated with operating rules based on a preferred alternative: an updated set of rule-curves for 14 major storage projects selected out of 6 alternatives evaluated to address the need for updated operations that integrate water management for anadromous fish habitat and survival (US Army Corps of Engineers, 2020).

Yakima regulation was simulated by USBR at a daily time step using the RiverWare model (Zagona et al., 2010). The Yakima regulation model was developed to simulate operations and irrigation under 2010 conditions (Bureau of Reclamation 2010b). Regulation in the Upper

Snake and Deschutes was modeled at a monthly time step using MODSIM (Labadie, 2006) to simulate operations and irrigation under 2008 conditions (Bureau of Reclamation 2009, 2010a).

Storage targets and outflows for all three hydro-regulation models vary inter-annually and year to year based on seasonal water supply forecasts and account for the interconnectedness of reservoirs across the system (RMJOC-II, 2020). The unregulated streamflow projections described in section 3.1 were input into the hydro-regulation models after adjustments were made to account for the effects of irrigation and reservoir evaporation. Irrigation and evaporation extractions were based on historical depletions for the period 1928-2008 and adjusted to the 2010 level of irrigation (Bonneville Power Administration, 2011). The resulting model output is an 80-member ensemble of regulated Columbia River basin streamflow projections for the RCP 8.5 emissions scenario.

4. Results

4.1 Seasonal Volumes

4.1.1 Regulation Significantly Dampens Unregulated Volume Changes in Winter (DJF) and Summer (JJA)

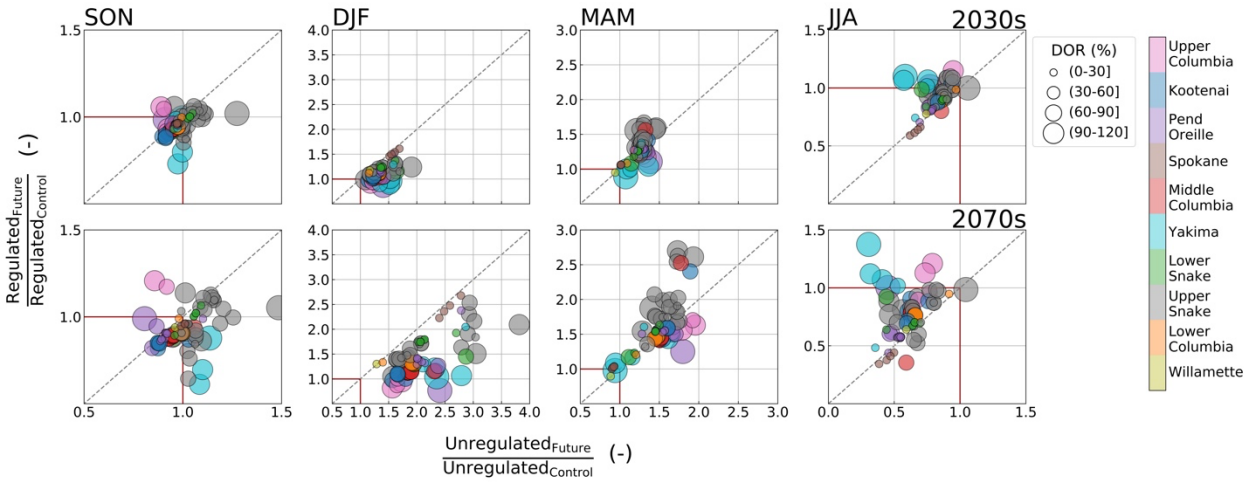

Figure 4. September-October (SON), December-February (DJF), March-May (MAM), and July-August (JJA) seasonal volume ratios for the 2030s (top) and 2070s (bottom) under unregulated conditions (x-axis) and regulated conditions (y-axis). Figure shows the median ratio across the 80-member ensemble. Points are colored by region and sized by the degree of upstream regulation (DOR). In the absence of regulation, points would fall on the dashed 1:1 line. The red box helps to identify the direction of change over time. Points within the red box indicate decreases in future volumes. Points outside of the box indicate increases in future volumes.

We investigate projected seasonal volume changes by taking the ratio of future volumes to control period volumes and compare ratios under unregulated and regulated conditions (Figure 4). Results show changes across all seasons for both conditions by the 2030s and 2070s, with the largest shifts occurring by the 2070s. We limit discussion of seasonal volume results to the 2070s, when the greatest changes and differences between unregulated and regulated outcomes occur.

Autumn (SON) unregulated volumes experience the least change (generally less than 25% change across locations) and the direction of change varies spatially. The greatest

unregulated seasonal changes occur in winter (DJF) due to increases in precipitation and more cool-season precipitation falling as rain rather than snow. The unregulated winter signal is strongest in headwater tributaries of the Pend Oreille, Yakima, Spokane, Upper Snake, and Lower Snake subbasins where the hydrologic regime shifts from snow to transient or transient to rain. Spring (MAM) unregulated volumes also increase significantly. Snow-dominant sites of the Upper Columbia, Kootenai, and Upper Snake see the largest increases in spring volumes (greater than 90% change) as warming temperatures shift snowmelt timing toward earlier in the water year. In the summer (JJA), unregulated volumes are projected to decrease across all locations. The summer months are historically water limited. Shifts in snowmelt timing coupled with warmer and drier summers drive large reductions in snowmelt-driven streamflow. The greatest reductions in summer occur at locations in the Yakima, Spokane, Lower Snake, and Pend Oreille where snow dominant regimes shift to transient by the 2070s (greater than 50% percent change).

The effects of regulation vary spatially in autumn and spring. Unregulated autumn volumes in upstream sites of the Upper Columbia (MCD and RVC) decrease by 8-14% but augmentation effects under regulation result in increases of 17-20%, respectively. These strong regulation effects diminish downstream. The opposite effects occur in the Yakima and Upper Snake, but most significantly in the Yakima. Except for a single location in the Yakima, unregulated autumn volumes increase by 2-13% where regulated volumes decrease by 4-38%. In the spring, sites in the Upper Snake that transition from snow-dominant to transient exhibit the greatest differences between changes in unregulated and regulated spring volumes where regulation amplifies changes (greater change relative to the control period).

In the winter and summer, regulation generally results in reduced change. Unregulated winter volumes are projected to increase by over 200% at some locations; however, regulation

significantly dampens these changes (less change relative to the control period) where upstream regulation (DOR) is greater than 30%. Many locations show large unregulated winter volume increases but no projected change or decreases under regulation. These effects predominantly occur in headwater reservoirs in the Upper Columbia, Kootenai, and Pend Oreille that are snow-dominant well into the future or remain snow dominant through the 2030s and have large DOR. For example, at Hungry Horse in the Pend Oreille subbasin, unregulated winter volumes increase by 140% but regulation results in a 23% decrease in winter volumes. Generally, strong winter regulation effects diminish downstream of headwater reservoirs. As in winter, summer regulation results in significant dampening of the climate signal in headwater reservoirs where DOR is large. For some locations, for example in headwaters of the Yakima and in the Upper Columbia, summer low flow augmentation not only dampens the climate signal, but results in increases in the regulated flow volume compared to decreases in the unregulated volume.

4.1.2 Level of Seasonal Volume Regulation Explains Large Regulation Effects in Winter (DJF) and Summer (JJA)

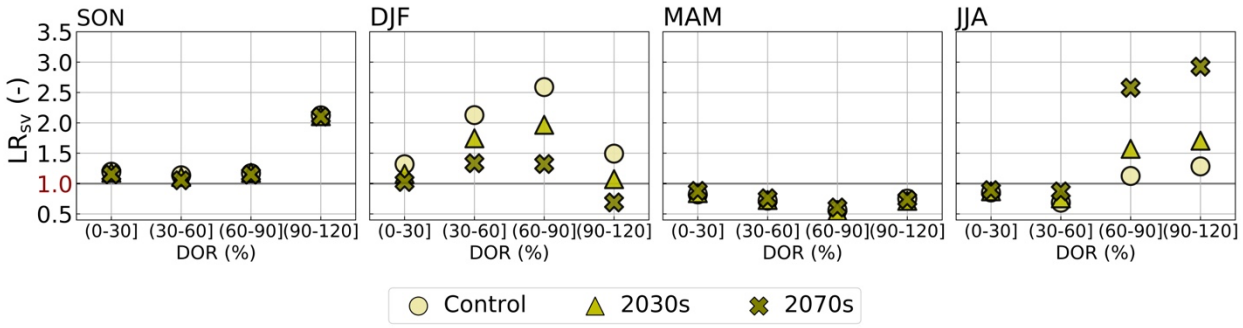

Figure 5. September-October (SON), December-February (DJF), March-May (MAM), and July-August (JJA) level of seasonal volume regulation (LRsv) across each period. LRsv is defined as the ratio of the regulated to unregulated seasonal volume. The figure shows the median LRsv from the 80-member ensemble. Ratios for each location have been grouped by the degree of upstream regulation (DOR) and averaged across each period. The lightest point shows the control period LRsv and the darkest point shows the 2070s LR_{SV}.

In section 4.1.1, we showed that seasonal volumes are projected to change under both unregulated and regulated conditions; however, regulation effects on the magnitude and direction of change vary widely across seasons. Much of this can be explained by seasonally varying operations that alter flow timing and the seasonality of the annual hydrograph. Figure 5 shows the effects of seasonally varying operations on unregulated flow volumes and how these effects are projected to change in the future.

Spring (MAM) straddles the period of the strong snowmelt pulse which typically occurs late spring/early summer. Streamflow across the basin is primarily snowmelt driven and control period peak flows typically occur during the spring freshet (see Figure 1). In the spring, reservoirs begin refilling (storing large volumes of water) for spring flood risk management and LR_{sv} (Eq. 2) is less than 1, because regulated flow volumes are less than unregulated flow volumes. Stored spring volumes are used to augment dry season low flows, and winter drafting drain reservoirs in preparation for the next spring freshet. Control period LR_{sv} is greater than 1 across autumn (SON), winter (DJF), and summer (JJA) (for locations where DOR is > 60%), and the largest LR_{sv}-values occur during winter drafting.

By the 2070s, large changes in the LR_{sv} occur in winter and summer when regulation effects on volume changes exhibit the strongest patterns (widespread dampening effects in winter and summer). Unregulated winter volumes are projected to increase significantly; however, as the system is operated to maintain control period conditions, regulated volume changes are relatively smaller and LR_{sv} approaches unity. In the summer, future unregulated volumes are projected to decrease. Like winter, the system is operated to maintain control period conditions and flow augmentation in the future results in less change under regulation. As a result, LR_{sv}-values exceed 1 where DOR is large.

4.2 Q50RP Ratios

4.2.1 Large Regulation Effects on Q50RP Flow Changes Occur in Headwater Tributary Sites Where DOR is Large

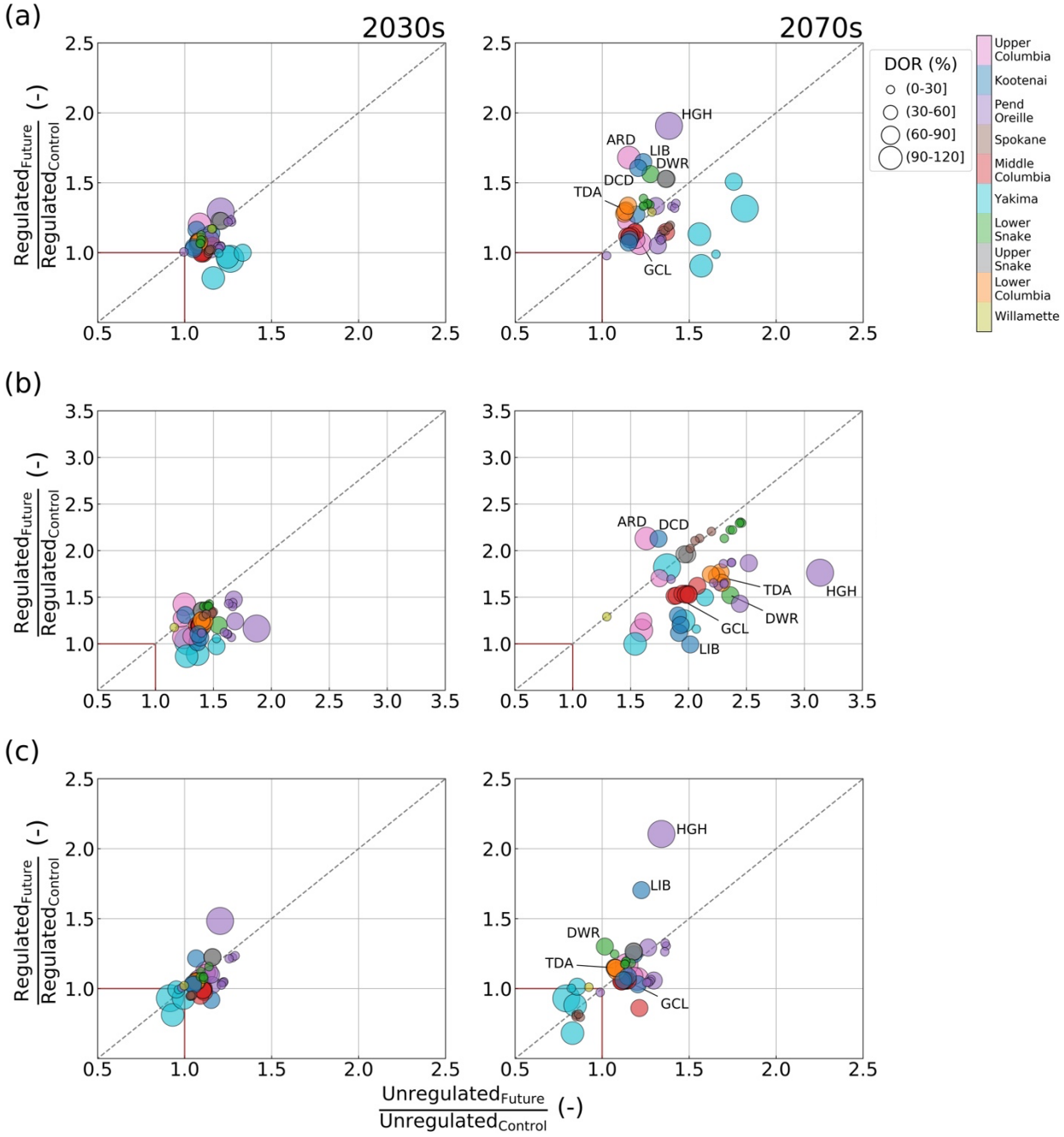

Figure 6. Annual (a), October-March (b), and April-September (c) 50-year return period peak flow ratios for unregulated conditions (x-axis) and regulated conditions (y-axis). Figure shows the median ratio across the 80-member ensemble. Points are colored by region and sized by the

degree of upstream regulation (DOR). In the absence of regulation, points would fall on the dashed 1:1 line. The red box helps to identify the direction of change over time. Points within the red box indicate decreases in future Q50 flows. Points outside of the box indicate increases in future Q50 flows. Sites that see significant differences between regulated and natural conditions are annotated. Also annotated are Grand Coulee (GCL) and The Dalles (TDA), located on the mainstem of the Middle Columbia and Lower Columbia, respectively.

Annual Q50RP flows are projected to increase by the 2070s across the domain (Figure 6a). The largest unregulated increases occur in the Yakima, Pend Oreille, Spokane, and Upper Snake subbasins (ordered from greatest increase to least). For the Pend Oreille, the magnitude of change is dependent on location in the river network (Figure A-4 of Appendix A). The effects of regulation vary spatially. Regulation significantly dampens changes in the Yakima and Spokane, tributaries where the hydrologic regimes shift to rain-dominant by the 2070s. Regulation amplifies Q50RP changes for a number of locations across the domain. The greatest amplification effects occur at upper elevation headwater reservoirs in the Pend Oreille (Hungry Horse; HGH), Kootenai (Libby; LIB, Duncan; DCD), and Lower Snake (Dworshak; DWR). Strong regulation effects also occur at Arrow Lakes (ARD), a high elevation reservoir in the Upper Columbia. Amplification effects from these reservoirs diminish downstream where large dampening effects occur, particularly in the Kootenai and Upper Columbia (Table A-1 of Appendix A).

We take a closer look at seasonal Q50RP changes to determine whether differences in flow maxima between unregulated and regulated conditions are driven by changes in the cool or warm season. During the cool season, unregulated Q50RP flows are projected to increase across the domain as a result of enhanced winter extremes and increased winter precipitation (Figure 6b). Regulated Q50RP flows are also projected to increase; however, operations result in significantly less change where DOR is greater than 30%. Some of the greatest dampening effects occur at Hungry Horse, Libby, and Dworshak. By the 2070s, regulation at Libby results

in no cool-season change. At Arrow Lakes and Duncan, 2070s cool-season unregulated Q50RP flows show increases of 63% and 74%, respectively; however, regulation amplifies these changes to 112% at both sites.

The warm season is a period when peak flows are driven by the spring freshet and climate change impacts during this period are spatially variable (Figure 6c). Warm-season unregulated Q50RP is projected to decrease by the 2070s for regions that exhibit rain-dominant regimes (Willamette, Spokane, and Yakima). Increases are projected for all other locations. Regulation generally follows changes in unregulated Q50RP. Exceptions occur at Hungry Horse, Libby, and Dworshak, where warm-season regulation results in an amplified climate signal.

Arrow Lakes and Duncan remain snow dominant through the 2070s, yet regulation dampens the warm season signal and amplifies the cool season signal indicating that annual amplification effects are driven by cool-season increases in regulated flows. Hungry Horse, Libby, and Dworshak see amplification effects in the warm season, indicating that annual amplification effects are driven by warm-season increases in regulated flows. These effects are also reflected in regulated peak flow timing changes shown in Figure A-6 of Appendix A.

4.2.2 Level of Q50RP Regulation Shows Regulation Has Little Effect on Warm-Season Q50RP Changes

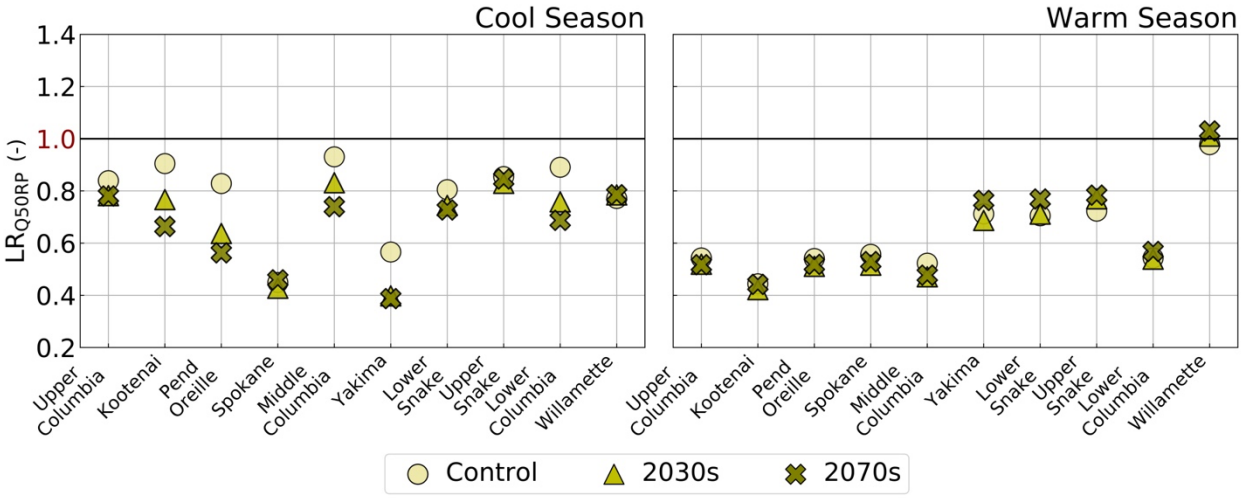

Figure 7. Seasonal level of regulation for the cool season (October-March) and warm season (April-September) where LR_{Q50RP} (y-axis) is the level of regulation defined as the ratio of regulated to unregulated Q50RP (Eq. 3). The figure shows the median LR_{Q50RP} from the 80-member ensemble. Ratios at each location have been grouped by the degree of upstream regulation (DOR) and averaged across region.

Figure 7 shows the level of Q50RP regulation (LR_{Q50RP}) (Eq. 3) averaged by region for the cool season and the warm season. Across seasons and regions, LR_{Q50RP} remains less than 1 in the future indicating that as the unregulated Q50RP increases the system still reduces future peaks relative to the unregulated flows (also shown in Figure A-5 of Appendix A). However, regulated Q50RP will generally increase relative to control period regulated Q50RP (Figure 6). The largest unregulated increases occur in the cool season and LR_{Q50RP}-values decrease (regulated Q50RP is significantly less than unregulated Q50RP in the future) indicating the system is largely reducing cool-season unregulated floods. In contrast, warm season LR_{Q50RP}-values show little change or increases in the future (as unregulated Q50RP flow increases, regulated Q50RP flow also increases), indicating that regulation has little effect on the climate signal for spring Q50RP changes.

4.3 7Q10 Low Flow Ratios

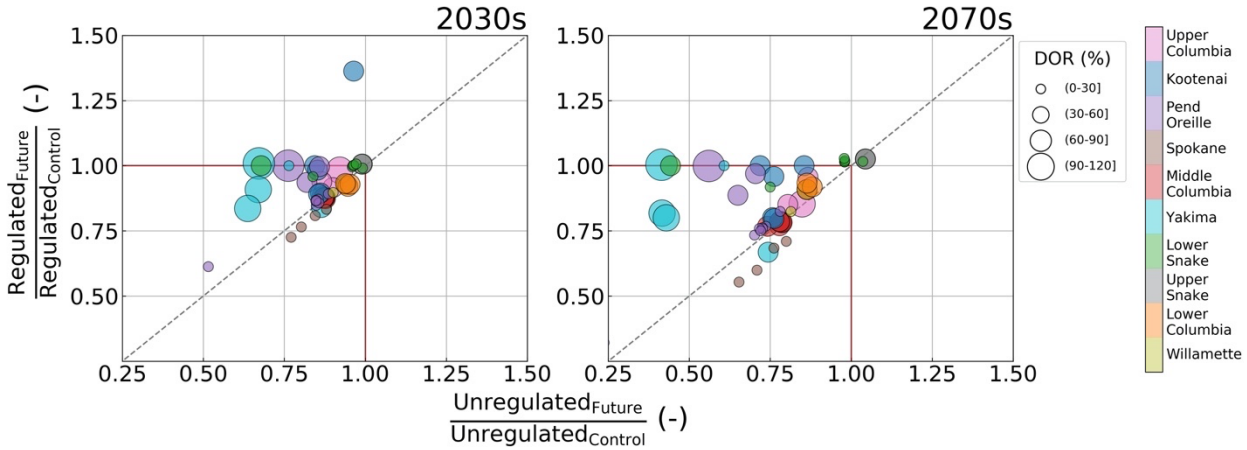

Figure 8. July-October 10-year return period 7-day average minimum flow (7Q10) ratios for unregulated conditions (x-axis) and regulated conditions (y-axis). Figure shows the median ratio across the 80-member ensemble. Points are colored by region and sized by the degree of upstream regulation (DOR). In the absence of regulation, points would fall on the dashed 1:1 line. The red box helps to identify the direction of change over time. Points within the red box indicate decreases in future 7Q10 flows. Points outside of the box indicate increases in future 7Q10 flows. For the 2070s, a single site in the Pend Oreille subbasin is not shown and exhibits a 76% decrease in 7Q10 flows.

7Q10 low flows are projected to decrease by both the 2030s and the 2070s under unregulated conditions across most sites (Figure 8). By the 2070s, the largest decreases occur in the Pend Oreille, Yakima, and Lower Snake subbasins where regimes shift from snow-dominant to transient or transient to rain-dominant. 7Q10 flows in the Yakima decrease by over 50%. Generally, under regulation, many sites are sensitive to the low flow signal. Exceptions occur in headwater tributaries of the Kootenai, Pend Oreille, Yakima, and Lower Snake subbasins. For the Spokane, regulation amplifies decreases in 7Q10. Like results for Q50RP, large regulation effects diminish downstream. On the mainstem, regulation is susceptible to the climate signal showing little to no difference from unregulated changes.

5. Discussion

Seasonally, regulation significantly dampens volume changes in the winter and summer where DOR is greater than 30%. Unregulated seasonal volume changes are largest in winter, a period when precipitation is projected to increase the most and warmer temperatures result in more cool-season precipitation falling as rain rather than snow. All locations show increases in unregulated winter volumes and there is strong agreement across the ensemble in the direction of change (Table A-2 of Appendix A). Under regulated conditions, winter volumes generally increase but reservoir operations dampen the magnitude of change. In the summer, warmer and drier conditions drive decreases in unregulated volumes, and, like winter, models agree on the direction of summer change (Table A-4 of Appendix A). Regulation generally dampens summer volume changes and sites with very large DOR show increases in volumes due to summer flow augmentation.

These results align with other studies that have investigated regulation effects on changing conditions in the Columbia River basin. Zhou et al. (2018) examined regulation effects on the timing of climate signal emergence (defined by the timing of hydrologic regime shifts) across the western US. Regulation effects in the Columbia River basin showed high seasonal dependence and delayed the timing of climate signal emergence during winter and summer at locations with a high level of regulation. Jones and Hammond (2020) investigated trends in historical inflows and outflows for large reservoirs across the basin and found that during the dry season, inflows to reservoirs decreased while outflows increased due to the effects of low flow augmentation.

The seasonal dependence of regulation effects can be explained by seasonally varying operations and projected future hydroclimate. Seasonal reservoir storage and the delayed release

of inflows alter streamflow timing. Reservoirs store large spring and summer volumes that are later used to augment late summer/early fall flows and then released throughout winter in preparation for the next spring freshet. This delayed release results in summer, fall, and winter reservoir outflows that exceed unregulated flows (Figure 5). As unregulated summer volumes decrease, the system operates to maintain control period conditions and releases more water in the future to augment low summer volumes resulting in dampening of the summer climate signal and, also, reservoirs that are less full by winter. In the winter, as unregulated volumes increase in the future, less full reservoirs have greater capacity to store increasing volumes and changes under regulation are relatively small resulting in a dampened winter signal. Regulation dampens or reverses the direction of winter volume changes at upper elevation headwater reservoirs that remain snow dominant in the future. Even under warming, these locations experience precipitation falling as snow rather than rain (RMJOC-II, 2018) resulting in relatively small unregulated volume changes and, consequently, greater capacity to mitigate winter changes.

The results for autumn and spring vary spatially. Unlike projections for the winter and summer, flow projections for the autumn and spring exhibit uncertainty in the direction of change across the ensemble (Tables A-1 and A-3 of Appendix A) driven by large uncertainty in precipitation patterns (RMJOC-II, 2018). Nevertheless, results for autumn and spring can be explained by the seasonality of operations. Autumn regulated volumes decrease in the Yakima where little to no change occurs for unregulated volumes. The annual hydrograph for Keechelus (KEE) (Figure 1), a headwater reservoir on the Yakima River, reflects large augmentation of future summer flows. Greater storage releases in the summer result in less storage by autumn and consequently, decreases in future autumn outflows. In the spring, the effects of regulation vary depending on hydroclimate and site-specific operational constraints. The spring months (MAM)

straddle the onset of the spring refill period. As the spring snowmelt pulse shifts earlier, reservoirs that historically empty through late spring could experience an amplification of spring changes if large volumes that occurred early summer during reservoir refill shift to late spring during periods of drafting.

Annual high flow extremes are projected to increase for unregulated conditions across the domain. This is in agreement with other studies that used the same unregulated flow dataset to investigate changes in future extremes (Chegwidden et al., 2020; Queen et al., 2019). Salathé et al. (2014) and Tohver et al. (2014) also projected widespread increases in high flow extremes across the Pacific Northwest, although these studies did not project increases across the entire domain. Regulation studies for large river basins in East Asia found that reservoir operations dampened changes in high flow extremes (Dong et al., 2019; Wang et al., 2017; Yun et al., 2021). In contrast, our study finds that regulation results in both dampening and amplification effects on high flow extremes depending on location in the river network and hydroclimate. Headwater reservoirs at upper elevations with large DOR exhibit amplification of annual extreme changes. In other words, regulated flows from large headwater reservoirs are more sensitive to shifts in extremes than unregulated flows. Although, not in the context of extreme flows, the phenomenon of large reservoirs exhibiting greater sensitivity to climate change has been discussed before. Zhou et al. (2018) found that basins with very large storage capacities are projected to be more sensitive to the climate signal, experiencing earlier shifts in the hydrologic regime relative to unregulated conditions. They explain this phenomenon to be the result of less variation in the seasonality of a "flattened-out" hydrograph under regulation. Small variations in outflow from large reservoirs during periods when streamflow is historically regulated can drive large amplification effects. For example, if a large reservoir releases less water after a high flow

extreme event in the past (historically low reservoir outflow after an unregulated high flow event) but releases more water after these events in the future, the changes under regulation can be large. Wang et al. (2017) found the opposite effects in the Lancang-Mekong River basin, where large reservoirs more effectively dampened extreme changes. They also found the largest regulation effects occur at upstream gages where DOR is large, and that these effects weaken downstream. Wang et al. (2017) argues that stronger regulation effects occur at upstream reservoirs due to relatively smaller annual discharge volumes. We show that the largest amplification effects of annual changes in high flow extremes occur at headwater reservoirs and generally diminish downstream where, in many cases, dampening occurs (Figure A-4 of Appendix A). Although regulation effects in the Columbia River basin contrast with Wang et al. (2017), our findings agree that the largest effects occur at headwater reservoirs where DOR is large. Reversal of regulation effects downstream (amplification upstream, dampening downstream) could be explained by the effects of operations. Headwater reservoirs will store more water during enhanced unregulated flood events thereby reducing the signal downstream. Water stored during these events is released (drafted) after the events, which could locally lead to future increases in high flows. These later releases could have less effect further downstream due to the compounding effects of the multi-reservoir network.

In the Upper Columbia, operations at Arrow Lakes and Duncan amplify the annual high flow extreme signal and these effects are driven by shifts in winter regulation (Figure 6b and Figure A-6 of Appendix A). The Upper Columbia remains snow-dominant in the 2070s. Regulation for this region dramatically flattens the annual hydrograph and exhibits two annual peaks in the winter and spring (Figure 1). Spring precipitation is projected to increase across the domain, which will lead to greater snowpack accumulation at upper elevations less sensitive to warming.

Spring reservoir storage targets for flood risk management are based on water supply forecasts derived from projected spring and summer snowpack (RMJOC-II, 2020). Increases in forecasted water supplies because of greater projected snowpack will result in greater spring storage needs for flood risk management. Winter drafting is paused during winter extreme events for flood risk management. The water stored during these events is later released in preparation for spring. Large increases in the magnitude of unregulated winter high flows combined with larger and earlier spring freshet could lead to greater releases after winter events at large upstream reservoirs. As previously discussed, small variations in large reservoir outflows could result in relatively large changes under regulation and amplification effects. The opposite seasonal effects occur at Hungry Horse, Libby, and Dworshak, headwater reservoirs in the Pend Oreille, Kootenai, and Lower Snake subbasins, respectively. Regulation at these sites amplifies the annual extreme signal driven by shifts in spring regulation (Figure 6c and Figure A-6 of Appendix A). Hydrologic regimes at Hungry Horse and Dworshak shift from snow-dominant to transient by the 2070s. Libby remains snow dominant but still shifts towards a more transient regime (Figure 2). Each of these reservoirs is operated for winter and spring flood risk management (RMJOC-II, 2020). In a transitional climate, more precipitation falling as rain rather than snow and large increases in the magnitude of winter flood events leads to fuller reservoirs at the end of the winter and less storage available to meet spring storage targets for flood risk management. Large regime shifts challenge the historically-based seasonal operational patterns of reservoir draft and refill, and regulated flows show greater sensitivity to spring extremes relative to unregulated conditions.

As previously stated, annual amplification effects under regulated conditions diminish downstream, where changes in unregulated flows are generally dampened under regulation. The

greatest dampening occurs in the winter when regulation reduces changes in winter high flow extremes. Annually, the largest reductions of high flow extremes occur for the Yakima and Spokane basins where regimes shift to rain-dominant in the future and, as a result, are mitigated by winter operations.

Although large changes in high flow extremes occur under both regulated and unregulated conditions, operations reduce unregulated floods into the future (Figure 7 and Figure A-5 of Appendix A). Significant reductions occur for winter floods. The system tends to exhibit greater sensitivity to changes in spring flood events which is likely the result of reservoirs already storing large volumes of water during the spring and, as a result, having less storage capacity to dampen increases in high flow extremes. Greater sensitivity and increases in regulated high flow extremes do not necessarily mean catastrophic flooding of riverbanks downstream. More work is needed to determine whether changes under regulation increase the likelihood of damaging flood events.

Unregulated July through October 7Q10 low flows are generally projected to decrease and the effects of regulation vary spatially. Some of the most significant reductions in low flow extremes occur in the Yakima and Spokane subbasins that exhibit shifts from transient to rain-dominant regimes in the future. Regulation mitigates large changes in the Yakima; however, regulation in the Spokane results in slight amplification effects. DOR is small in the Spokane, and the reservoir network consists primarily of run-of-river projects that have little to no storage capacity for water that can be used to augment low flows. Large dampening effects tend to occur in headwater tributaries of the Kootenai, Pend Oreille, and Lower Snake subbasins where upstream DOR is large. These locations have smaller annual streamflow volumes and consequently, large regulation effects on changes in low flow extremes.

6. Conclusion

Regulation modulates the seasonality of the annual hydrograph resulting in regulation effects that vary across time and across the basin. Reservoir operations dampen the climate signal for winter and summer at locations where DOR is large, but results for fall and spring vary widely across the domain depending on local operational constraints and hydroclimate. For both seasonal volumes and high flow extremes, the strongest regulation effects occur at headwater reservoirs where DOR is large. Large storage capacity coupled with smaller annual volumes result in strong regulation effects, but this behavior generally diminishes downstream. For high flow extremes, regulation at headwater reservoirs can amplify change. Slight variations in the seasonality of outflows from large reservoirs can result in large seasonal changes under regulation leading to amplification effects. Low flow extreme outcomes vary spatially. In general, the system exhibits sensitivity to low flow extremes following changes under unregulated conditions; however, for tributaries of the Kootenai, Pend Oreille, Yakima, and Lower Snake, augmentation dampens low flow changes.

Regulation dampens future changes in winter and summer volumes and winter high flow extremes; however, for most locations, operations are not able to restore control period conditions. Operations based on historical conditions are seasonally dependent and, for historically snow dominant headwater reservoirs, regulation dramatically reduces the seasonality of the annual hydrograph. At these locations, large seasonal shifts in hydroclimate result in greater sensitivity to high flow extreme changes under regulation. Operational rule-curves were developed based on the assumption of stationarity, which is no longer practical in a rapidly changing system (Milly et al., 2008). While this work shows that dams can be a useful tool for ameliorating the effects of climate change on streamflow, understanding how to use them

effectively requires further investigation. The basin's water resources will benefit from adaptable management measures that account for seasonal shifts in a warmer future climate.

References

Barnes, C. A., Duxbury, A. C., & Morse, B.-A. (1972). Circulation and selected properties of the Columbia River effluent at sea. In *The Columbia River Estuary and Adjacent Ocean Waters*, A.T. Pruter and D.L. Alverson.

Barnett, T. P., Adam, J. C., & Lettenmaier, D. P. (2005). Potential impacts of a warming climate on water availability in snow-dominated regions. *Nature, 438(7066)*, 303–309. https://doi.org/10.1038/nature04141

Beard, L.R. and Fredrich, A.J. (1975). Hydrologic Engineering Methods for Water Resources Development: Hydrologic Frequency Analysis Volume 3. https://www.hec.usace.army.mil/publications/IHDVolumes/IHD-3.pdf

Bonneville Power Administration. (2011). 2010 Level Modified Streamflow: 1928-2008. DOE/BP-4352, Portland, OR: Bonneville Power Administration. https://www.bpa.gov/p.Power-Products/Historical-Streamflow-Data/streamflow/2010-Level-Modified-Streamflow.pdf

Bureau of Reclamation. (2009). Naturalized and Modified Flows of the Deschutes River Basin. Boise, ID: Bureau of Reclamation, Pacific Northwest Regional Office.

Bureau of Reclamation. (2010a). Modified and Naturalized Flows of the Snake River Basin above Brownlee Reservoir. Boise, ID: Bureau of Reclamation, Pacific Northwest Regional Office.

Bureau of Reclamation. (2010b). Naturalized and Modified Flows of the Yakima River Basin, Columbia River Tributary, Washington. Yakima, WA: Bureau of Reclamation, Columbia-Cascades Area Office.

Bureau of Reclamation. (2016). Columbia River Basin: Climate Impact Assessment, (March), 301pp.

Chegwidden, O. S., Nijssen, B., Rupp, D. E., and Mote, P. W.: Hydrologic Response of the Columbia River System to Climate Change, Zenodo, https://doi.org/10.5281/zenodo.854763, 2017.

Chegwidden, O. S., Nijssen, B., Rupp, D. E., Arnold, J. R., Clark, M. P., Hamman, J. J., et al. (2019). How Do Modeling Decisions Affect the Spread Among Hydrologic Climate Change Projections? Exploring a Large Ensemble of Simulations Across a Diversity of Hydroclimates. *Earth's Future, 7(6)*, 623–637. https://doi.org/10.1029/2018EF001047

Chegwidden, O. S., Rupp, D. E., & Nijssen, B. (2020). Climate change alters flood magnitudes and mechanisms in climatically-diverse headwaters across the northwestern United States. *Environmental Research Letters, 15(9).* https://doi.org/10.1088/1748-9326/ab986f

Chowdhury, J. U., & Stedinger, J. R. (1991). Confidence interval for design floods with estimated skew coefficient. *Journal of Hydraulic Engineering, 117(7)*, 811–831. https://doi.org/10.1061/(ASCE)0733-9429(1991)117:7(811)

Cohn, T. A., England, J. F., Berenbrock, C. E., Mason, R. R., Stedinger, J. R., & Lamontagne, J. R. (2013). A generalized Grubbs-Beck test statistic for detecting multiple potentially influential low outliers in flood series. *Water Resources Research, 49(8*), 5047–5058. https://doi.org/10.1002/wrcr.20392

Dong, N., Yu, Z., Gu, H., Yang, C., Yang, M., Wei, J., et al. (2019). Climate-induced hydrological impact mitigated by a high-density reservoir network in the Poyang Lake Basin. *Journal of Hydrology, 579(June)*, 124148. https://doi.org/10.1016/j.jhydrol.2019.124148

Dynesius, M., & Nilsson, C. (1994). Fragmentation and flow regulation of river systems in the northern third of the world. *Science, 266(5186),* 753–762. https://doi.org/10.1126/science.266.5186.753

Elsner, M. M., Cuo, L., Voisin, N., Deems, J. S., Hamlet, A. F., Vano, J. A., et al. (2010). Implications of 21st century climate change for the hydrology of Washington State. *Climatic Change, 102(1–2)*, 225–260. https://doi.org/10.1007/s10584-010-9855-0

England, J.F., Jr., Cohn,T.A., Faber,B.A., Stedinger, J.R., Thomas, W.O., Jr., Veilleux, A.G., Kiang, J.E., and Mason, R.R., J. (2018). Guidelines for Determining Flood Flow Frequency Bulletin 17C Book 4, Hydrologic Analysis and Interpretation Techniques and Methods 4-B5. Retrieved from https://pubs.usgs.gov/tm/04/b05/tm4b5.pdf

England, J.F., Jr. & Cohn,T.A. (2019). PeakfqSA Software. https://sites.google.com/a/alumni.colostate.edu/jengland/bulletin-17c#Software

Esri. (2009). "World Physical Map." https://services.arcgisonline.com/ArcGIS/rest/services/World_Physical_Map/MapServer

Esri. (2011). "World Light Gray Reference." https://services.arcgisonline.com/ArcGIS/rest/services/Canvas/World_Light_Gray_Reference/MapServer

Frans, C., Istanbulluoglu, E., Lettenmaier, D. P., Fountain, A. G., & Riedel, J. (2018). Glacier Recession and the Response of Summer Streamflow in the Pacific Northwest United States, 1960–2099. *Water Resources Research, 54(9)*, 6202–6225. https://doi.org/10.1029/2017WR021764

Fritze, H., Stewart, I. T., & Pebesma, E. (2011). Shifts in Western North American Snowmelt Runoff Regimes for the Recent Warm Decades. *Journal of Hydrometeorology, 12(5)*, 989–1006. https://doi.org/10.1175/2011JHM1360.1

Gergel, D. R., Nijssen, B., Abatzoglou, J. T., Lettenmaier, D. P., & Stumbaugh, M. R. (2017). Effects of climate change on snowpack and fire potential in the western USA. *Climatic Change, 141(2)*, 287–299. https://doi.org/10.1007/s10584-017-1899-y

Grill, G., Lehner, B., Thieme, M., Geenen, B., Tickner, D., Antonelli, F., et al. (2019). Mapping the world's free-flowing rivers. *Nature, 569(7755)*, 215–221. https://doi.org/10.1038/s41586-019-1111-9

Hamlet, A. F., & Lettenmaier, D. P. (2007). Effects of 20th century warming and climate variability on flood risk in the western U.S. *Water Resources Research, 43(6)*, 1–17. https://doi.org/10.1029/2006WR005099

Hamlet, A. F., Lee, S. Y., Mickelson, K. E. B., & Elsner, M. M. (2010). Effects of projected climate change on energy supply and demand in the Pacific Northwest and Washington State. *Climatic Change, 102(1–2)*, 103–128. https://doi.org/10.1007/s10584-010-9857-y

Helsel, D. R., Hirsch, R. M., Ryberg, K. R., Archfield, S. A., & Gilroy, E. J. (2020). Statistical Methods in Water Resources Techniques and Methods 4 – A3. USGS Techniques and Methods.

IPCC. (2014). Climate Change 2014 Synthesis Report Summary Chapter for Policymakers. IPCC, 31. https://doi.org/10.1017/CBO9781107415324

Jennings, M. E., & Benson, M.A. (1969). Frequency curves for annual flood series with some zero events or incomplete data. *Water Resources Research, 5(1)*, 276–280.

Jones, J. A., & Hammond, J. C. (2020). River management response to multi-decade changes in timing of reservoir inflows, Columbia River Basin, USA. *Hydrological Processes, 34(25)*, 4814–4830. https://doi.org/10.1002/hyp.13910

Kammerer, J. C. (1990). Largest rivers in the United States. Open-File Report, (May), 2. Retrieved from http://pubs.usgs.gov/of/1987/ofr87-242/pdf/ofr87242.pdf

Labadie, J. W. (2006). MODSIM: Decision support system for integrated river basin management. Proceedings of the IEMSs 3rd Biennial Meeting, "Summit on Environmental Modelling and Software".

Leavesley, G. H., Lichty, R. W., Troutman, B. M., & Saindon, L. G. (1983). Precipitation-runoff modeling system—User's manual. U.S. Geological Survey Water-Resources Investigations Report, 83(4238), 207.

Lee, S. Y., Hamlet, A. F., & Grossman, E. E. (2016). Impacts of Climate Change on Regulated Streamflow, Hydrologic Extremes, Hydropower Production, and Sediment Discharge in the Skagit River Basin. *Northwest Science, 90(1)*, 23–43. https://doi.org/10.3955/046.090.0104

Lee, S., Won, J., Binder, L. W., & Lott, F. (2018). Effect of Climate Change on Flooding in King County Rivers: Using New Regional Climate Model Simulations to Quantify Changes in Flood, (May).

Lehner, B., Liermann, C. R., Revenga, C., Vörömsmarty, C., Fekete, B., Crouzet, P., et al. (2011). High-resolution mapping of the world's reservoirs and dams for sustainable river-flow management. *Frontiers in Ecology and the Environment, 9(9)*, 494–502. https://doi.org/10.1890/100125

Leppi, J. C., DeLuca, T. H., Harrar, S. W., & Running, S. W. (2012). Impacts of climate change on August stream discharge in the Central-Rocky Mountains. *Climatic Change, 112(3–4)*, 997–1014. https://doi.org/10.1007/s10584-011-0235-1

Li, H., Wigmosta, M. S., Wu, H., Huang, M., Ke, Y., Coleman, A. M., & Leung, L. R. (2013). A physically based runoff routing model for land surface and earth system models. *Journal of Hydrometeorology, 14(3)*, 808–828. https://doi.org/10.1175/JHM-D-12-015.1

Liang, X., Lettenmaier, D. P., Wood, E. F., & Burges, S. J. (1994). A simple hydrologically based model of land surface water and energy fluxes for general circulation models. *Journal of Geophysical Research, 99(D7)*. https://doi.org/10.1029/94jd00483

Lute, A. C., Abatzoglou, J. T., & Hegewisch, K. C. (2015). Projected changes in snowfall extremes and interannual variability of snowfall in the western United States. *Water Resources Research*. https://doi.org/10.1002/2014WR016267

Mantua, N., Tohver, I., & Hamlet, A. (2010). Climate change impacts on streamflow extremes and summertime stream temperature and their possible consequences for freshwater salmon habitat in Washington State. *Climatic Change, 102(1–2)*, 187–223. https://doi.org/10.1007/s10584-010-9845-2

May C., Luce, C., Casola, J., Chang, M., Cuhaciyan, J., Dalton, M., et al. (2018). Chapter 24. Northwest. Impacts, Risks, and Adaptation in the United States: Fourth National Climate Assessment, Volume II [Reidmiller, D.R., C.W. Avery, D.R. Easterling, K.E. Kunkel, K.L.M. Lewis, T.K. Maycock, and B.C. Stewart (Eds.)], II, 1036–1100. https://doi.org/10.7930/NCA4.2018.CH24

Milly, P. C. D., Betancourt, J., Falkenmark, M., Hirsch, R. M., Kundzewicz, Z. W., Lettenmaier, D. P., & Stouffer, R. J. (2008). Climate change: Stationarity is dead: Whither water management? *Science, 319(5863)*, 573–574. https://doi.org/10.1126/science.1151915

Moore, R. D., Pelto, B., Menounos, B., & Hutchinson, D. (2020). Detecting the Effects of Sustained Glacier Wastage on Streamflow in Variably Glacierized Catchments. *Frontiers in Earth Science, 8(May)*. https://doi.org/10.3389/feart.2020.00136

Musselman, K. N., Lehner, F., Ikeda, K., Clark, M. P., Prein, A. F., Liu, C., et al. (2018). Projected increases and shifts in rain-on-snow flood risk over western North America. *Nature Climate Change, 8(9)*, 808–812. https://doi.org/10.1038/s41558-018-0236-4

Payne, J., Wood, A., & Hamlet, A. (2004). Mitigating the effects of climate change on the water resources of the Columbia River basin. *Climatic Change, 62(1–3)*, 233–256. https://doi.org/10.1023/B:CLIM.0000013694.18154.d6

Queen, L. E., Mote, P. W., Rupp, D. E., Chegwidden, O., & Nijssen, B. (2021). Ubiquitous increases in flood magnitude in the Columbia River basin under climate change. *Hydrology and Earth System Sciences, 25(1)*, 257–272. https://doi.org/10.5194/hess-25-257-2021

Reidmiller, D.R., Avery, C.W., Easterling, D.R., Kunkel, K.E., Lewis, K.L.M., Maycock, T.K., and Stewart, B.C. (2018). Impacts, Risks, and Adaptation in the United States: Fourth National Climate Assessment. USGCRP Volume II, https://doi.org/10.7930/NCA4.2018

RMJOC-II (River Management Joint Operating Committee). (2018). Climate and hydrology datasets for RMJOC long-term planning studies: Second Edition (RMJOC-II) Part I: Hydroclimate projections and analyses, (June).

RMJOC-II (River Management Joint Operating Committee). (2020). Climate and Hydrology Datasets for RMJOC Long-Term Planning Studies: Second Edition Part II: Columbia River Reservoir Regulation and Operations — Modeling and Analyses.

Rupp, D. E., Abatzoglou, J. T., & Mote, P. W. (2017). Projections of 21st century climate of the Columbia River Basin. *Climate Dynamics, 49(5–6)*, 1783–1799. https://doi.org/10.1007/s00382-016-3418-7

Salas, J. D., Kroll, C. N., Cancelliere, A., Fernández, B., Raynal, J. A., & Lee, D. R. (2019). Low Flows and Droughts. Statistical Analysis of Hydrologic Variables, 269–332. https://doi.org/10.1061/9780784415177.ch08

Salathé, E. P., Hamlet, A. F., Mass, C. F., Lee, S. Y., Stumbaugh, M., & Steed, R. (2014). Estimates of twenty-first-century flood risk in the Pacific Northwest based on regional climate model simulations. *Journal of Hydrometeorology, 15(5)*, 1881–1899. https://doi.org/10.1175/JHM-D-13-0137.1

Stedinger, J.R., Vogel, R.M., & Foufoula-Georgiou, E. (1993). Frequency Analysis of Extreme Events. Handbook of Hydrology, 18.1-18.6.

Stedinger, J.R., Griffis, V.W. (2008). Flood Frequency Analysis in the United States: Time to Update. *Journal of Hydrologic Engineering, 13(4)*, 199-204. doi:10.1061/(ASCE)1084-0699(2008)13:4(199)

Stern, C.V. (2020). Columbia River Treaty Review (R43287). Congressional Research Service.

Stewart, I. T., Cayan, D. R., & Dettinger, M. D. (2005). Changes toward earlier streamflow timing across western North America. *Journal of Climate, 18(8)*, 1136–1155. https://doi.org/10.1175/JCLI3321.1

Tohver, I. M., Hamlet, A. F., & Lee, S. Y. (2014). Impacts of 21st-Century Climate Change on Hydrologic Extremes in the Pacific Northwest Region of North America. *Journal of the American Water Resources Association, 50(6)*, 1461–1476. https://doi.org/10.1111/jawr.12199

U.S. Army Corps of Engineers (USACE), (2013). HEC-ResSim Reservoir System Simulation User's Manual Version 3.1, (May), 556.

U.S. Army Corps of Engineers (USACE) (2020). Columbia River System Operations Environmental Impact Statement Record of Decision. https://www.nwd.usace.army.mil/CRSO/Final-EIS/

Vano, J. (2015). Seasonal hydrologic responses to climate change in the Pacific Northwest. *Water Resources Research, 51*, 1959–1976. https://doi.org/10.1002/2014WR015909.Received

Veilleux, A.G., Cohn, T.A., Flynn, K.M., Mason, R.R., Jr., and Hummel, P.R., (2014). Estimating magnitude and frequency of floods using the PeakFQ 7.0 program: U.S. Geological Survey Fact Sheet 2013-3108, 2 p., https://dx.doi.org/10.3133/fs20133108

Voisin, N., Li, H., Ward, D., Huang, M., Wigmosta, M., & Leung, L. R. (2013). On an improved sub-regional water resources management representation for integration into earth system models. *Hydrology and Earth System Sciences Discussions, 10(3)*, 3501–3540. https://doi.org/10.5194/hessd-10-3501-2013

Wang, W., Lu, H., Ruby Leung, L., Li, H. Y., Zhao, J., Tian, F., et al. (2017). Dam Construction in Lancang-Mekong River Basin Could Mitigate Future Flood Risk From Warming-Induced Intensified Rainfall. *Geophysical Research Letters, 44(20)*, 10,378-10,386. https://doi.org/10.1002/2017GL075037

Warner, M. D., & Mass, C. F. (2017). Changes in the climatology, structure, and seasonality of northeast pacific atmospheric rivers in CMIP5 climate simulations. *Journal of Hydrometeorology, 18(8)*, 2131–2141. https://doi.org/10.1175/JHM-D-16-0200.1

Wood, A. W., Leung, L. R., Sridhar, V., & Lettenmaier, D. P. (2004). Hydrologic implications of dynamical and statistical approaches to downscaling climate model outputs. *Climatic Change, 62(1–3)*, 189–216. https://doi.org/10.1023/B:CLIM.0000013685.99609.9e

Yun, X., Tang, Q., Li, J., Lu, H., Zhang, L., & Chen, D. (2021). Science of the Total Environment Can reservoir regulation mitigate future climate change induced hydrological extremes in the Lancang-Mekong River Basin? *Science of the Total Environment, 785*, 147322. https://doi.org/10.1016/j.scitotenv.2021.147322

Zagona, E., Nowak, K., Rajagopalan, B., Carly, J., & Prairie, J. (2010). Riverware's Integrated Modeling and Analysis Tools for Long-Term Planning Under Uncertainty. 2nd Joint Federal Interagency Conference, 1–12.

Zhou, T., Voisin, N., Lenga, G., Huang, M., & Kraucunas, I. (2018). Sensitivity of regulated flow regimes to climate change in the western United States. *Journal of Hydrometeorology, 19(3)*, 499–515. https://doi.org/10.1175/JHM-D-17-0095.1

Appendix A

Table of Contents

List of Figures

List of Tables

A.1 Extreme Flow Frequency Methods

A.1.1 High Flow Frequency Methods

As recommended by Bulletin 17C (England et al., 2018), the Log Pearson Type III (LP3) distribution with the Expected Moments Algorithm (Stedinger and Griffis, 2008) method was used to fit distribution curves to annual and seasonal maximum time series. Distributions and 90% confidence intervals were computed using a USACE version of the Unites States Geological Survey (USGS) Peakfq flood frequency software (Veillus, et al. 2014). PeakfqSA is a stand-alone version of Peakfq for Linux and Windows operating systems (England and Cohn, 2019). PeakfqSA configuration file options were set to use the station (at-site) skew, the Multiple Grubbs Beck test (Cohn et al., 2013) to detect and adjust for low outliers, and the plotting position

$$p_{i:n} = \frac{i - \alpha}{n + 1 - 2\alpha} \quad (1)$$

where $\alpha = 0.4$ and n is the sample size of the data.

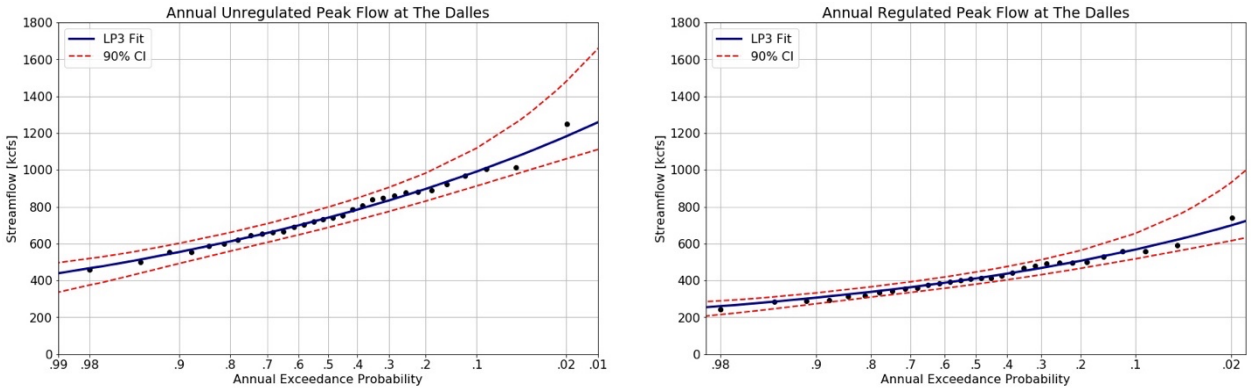

Figure A-1. LP3 PeakfqSA fits of The Dalles annual maxima for a single ensemble member. Shown are fits for unregulated (left) and regulated (right) for control period (1976-2005) maxima.

A.1.2 Low Flow Frequency Methods

The LP3 distribution with the method of moments was used to describe annual July through October 7-day average minimums. Calculation of the distribution and confidence intervals follow methods presented by Chowdhury and Stedinger (1991) and Stedinger et al. (1993). If X_p is the p^{th} quantile of the LP3 distribution, then

$$X_p = 10^{(\mu_y - K_p \sigma_y)}, \tag{2}$$

where μ_y and σ_y are the mean and standard deviation of the log-transformed sample y, respectively. K_p is approximated by the Wilson-Hilferty transformation.

$$K_p \approx \frac{2}{\gamma_m}\left(1 + \frac{\gamma_y z_p}{6} - \frac{\gamma_y^2}{36}\right)^3 - \frac{2}{\gamma}, \tag{3}$$

where γ_y is the skew of the log-transformed sample and z_p is the p^{th} quantile of the standard normal distribution.

For each LP3 fit, we calculate the 90% confidence bounds CI_{90} as

$$CI_{90} = X_p \pm \eta(\zeta_{0.05,p} - z_p)\sigma, \tag{4}$$

where σ is the standard deviation of the sample, and z_p is the p^{th} quantile of the standard normal distribution. $\zeta_{0.05,p}$ is the 5^{th} percentile of the noncentral t-distribution and estimated as

$$\zeta_{0.05,p} \approx \frac{z_p + z_{0.5}\sqrt{\frac{1}{n} + \frac{z_p^2}{2(n-1)} - \frac{z_{0.5}^2}{2n(n-1)}}}{1 - \frac{z_{0.5}^2}{2(n-1)}}, \tag{5}$$

where n is the sample size of the data and $z_{0.05}$ is the 5^{th} quantile of the standard normal distribution. z_p and $z_{0.05}$ were determined using the Python library scipy's normal percent point function: scipy.stats.norm.ppf(). η is a scaling factor to extend confidence intervals for normal quantiles to the Pearson Type III distribution and is estimated as

$$\eta \cong \sqrt{\frac{1 + \gamma K_p + \frac{1}{2}\left(1 + \frac{3}{4}\gamma^2\right)K_p^2}{1 + \frac{1}{2}z_p^2}}. \tag{6}$$

Time series of low flows may exhibit autocorrelation due to groundwater dependence. Autocorrelation in the sample impacts certainty that our data are drawn from the same distribution and, therefore, our goodness-of-fit. To address this, we determine the goodness-of-fit by testing for autocorrelation using Pearson's lag-1 autocorrelation test:

$$r_k = \frac{\sum_{t=k+1}^{n-k}(x_{t-k} - \bar{x})(x_t - \bar{x})}{\sum_{t=1}^{n}(x_t - \bar{x})^2}, \tag{7}$$

where k is the lag (in our case, $k = 1$) and n is the sample size. We used Python library scipy's pearson r function to determine r and corresponding confidence levels: scipy.stats.pearsonr(). If autocorrelation exists, we use the effective sample size (Dingman, 2015) to calculate confidence intervals, replacing n in equation (6) with n_{eff} defined as

$$n_{eff} = n\left(\frac{1 - r}{1 + r}\right). \tag{8}$$

Samples where zero-flows cannot be log-transformed require truncation. While the LP3 curve can be fit using truncated data parameters, this poses a problem for estimating the correct probabilities considering flows from the sample population could be zero. Jennings and Benson (1969) developed a method to estimate probabilities that account for zero flows for truncated data. This method is described by Salas et al. (2019), where the probability q that a given 7 day-minimum X is less than or equal to x_q is

$$P(X \leq x_q) = F(x_q) = q. \tag{9}$$

If a truncated sample has some number n_o of zero values, an estimator of the probability of a zero flow is

$$\hat{q}_0 = P(X = 0) = \frac{n_o}{n} \tag{10}$$

which can be used to adjust the probability q:

$$q_T = \frac{q - \hat{q}_0}{1 - \hat{q}_0}. \tag{11}$$

We use this method to adjust probabilities for sites and projections where zero flows are present.

After adjustments are made for zero flows, an issue still exists if $\hat{q}_0$ (eq 10) is greater than the probability of interest (in our case, the 0.1 percentile corresponding to a 10-year return period) due to truncation of the LP3 fit (Figure A-3a). In this special case, we fit the data non-parametrically by interpolating between each point of the sample. Following methods described by (Helsel et al., 2020), we determined non-parametric confidence intervals using the probabilities of the binomial distribution. The cumulative distribution function (cdf) of the binomial distribution is used to determine critical values using the sorted sample's rankings. Data from the sample that correspond to critical values are used as non-parametric confidence bounds. In our case, we computed the 90% confidence interval corresponding to 0.05 and 0.95 quantiles of the binomial cdf. The sample values associated with these rankings form the upper and lower confidence limits of the non-parametric fit.

Even in samples without zero flow values, time series that include near zero flows can exhibit poor LP3 fits. For this reason, we also used non-parametric methods to fit the distribution where more than 10% of the sample fell outside of the confidence intervals.

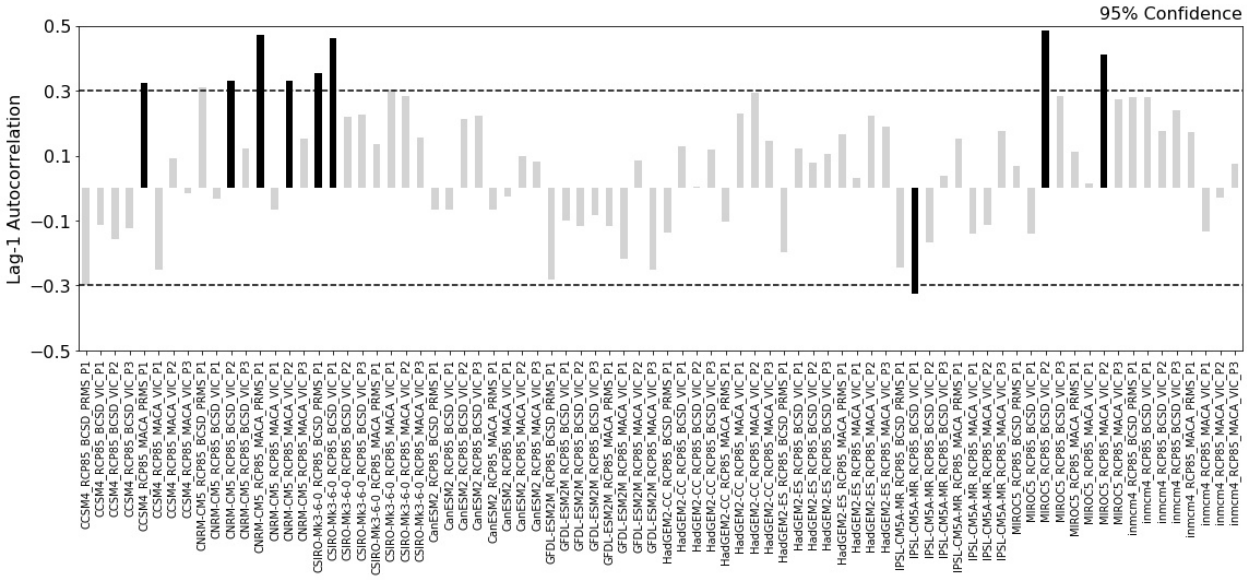

Figure A-2. Autocorrelation test results for 30-year 7-day minimum time series for a single site (Keechelus; KEE). Gray bars indicate time series that do not exhibit autocorrelation. Black bars indicate time series that exhibit autocorrelation with 95% confidence.

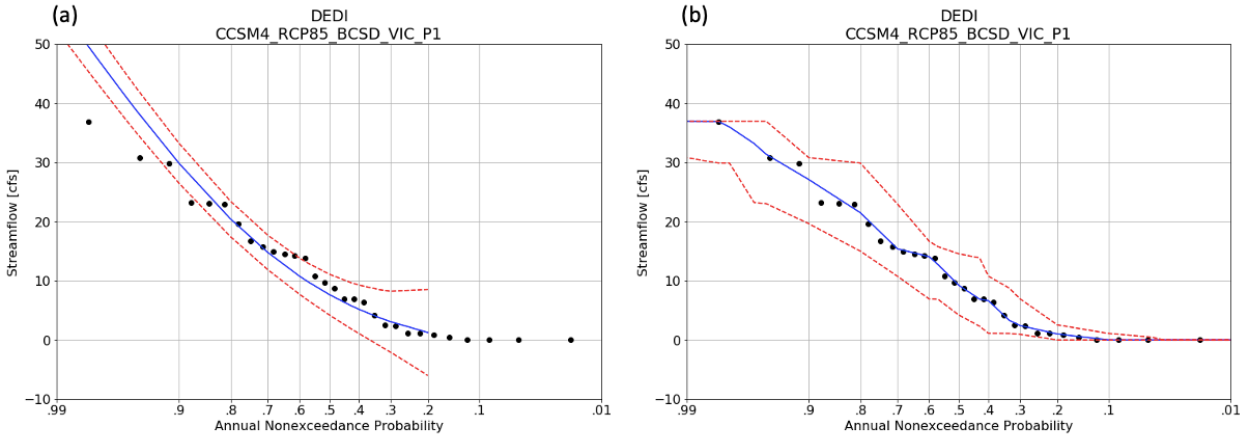

Figure A-3. LP3 low flow fit for truncated sample (a) and non-parametric fit (b) for a single site and ensemble member where zero flows exist for the 10% annual non-exceedance probability.

A.2 Annual Q50RP Percent Changes and Absolute Values

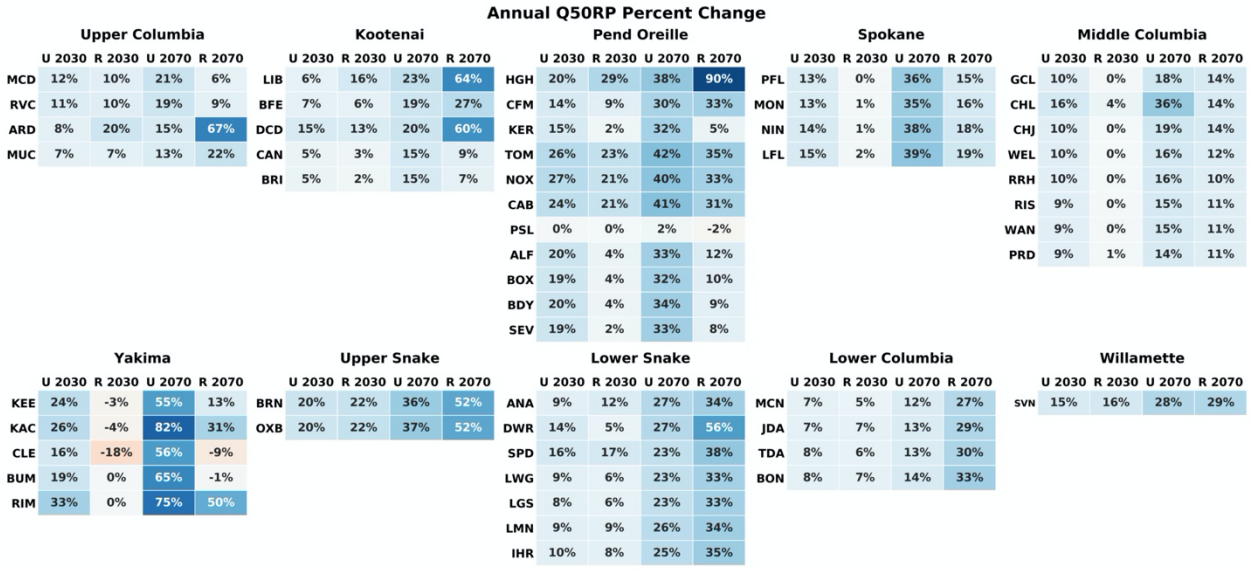

Figure A-4. Median percent change of annual Q50RP flow for unregulated conditions (U) and regulated conditions (R). For each region, locations are sorted from upstream (top) to downstream (bottom) based on position of tributary confluence with the next lowest order stream using a top-down stream order approach (e.g., a headwater tributary has a higher stream order than the mainstem).

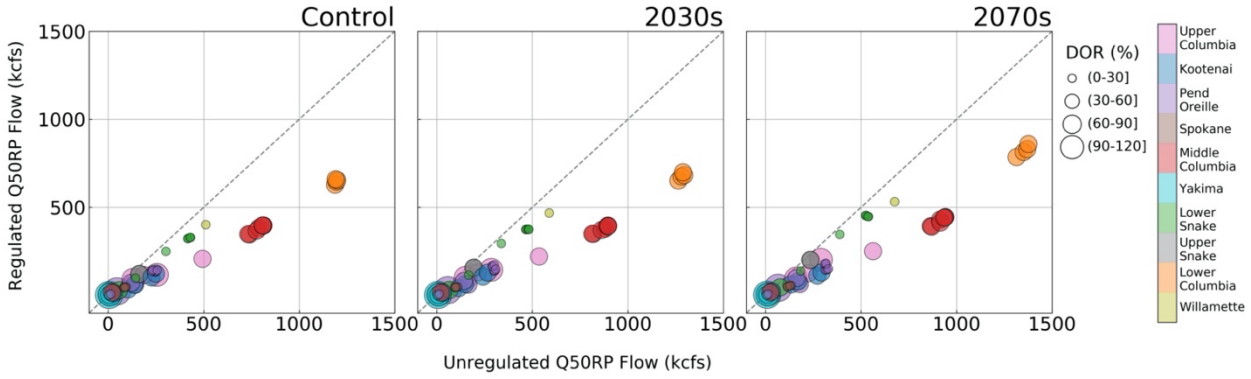

Figure A-5. Annual 50-year return period peak flows (Q50RP) for unregulated conditions (x-axis) and regulated conditions (y-axis). Figure shows the median Q50RP flows across the 80-member ensemble. Points are colored by region and sized by the degree of upstream regulation (DOR). In the absence of regulation, points would fall on the dashed 1:1 line.

A.3 Annual Maximum Timing

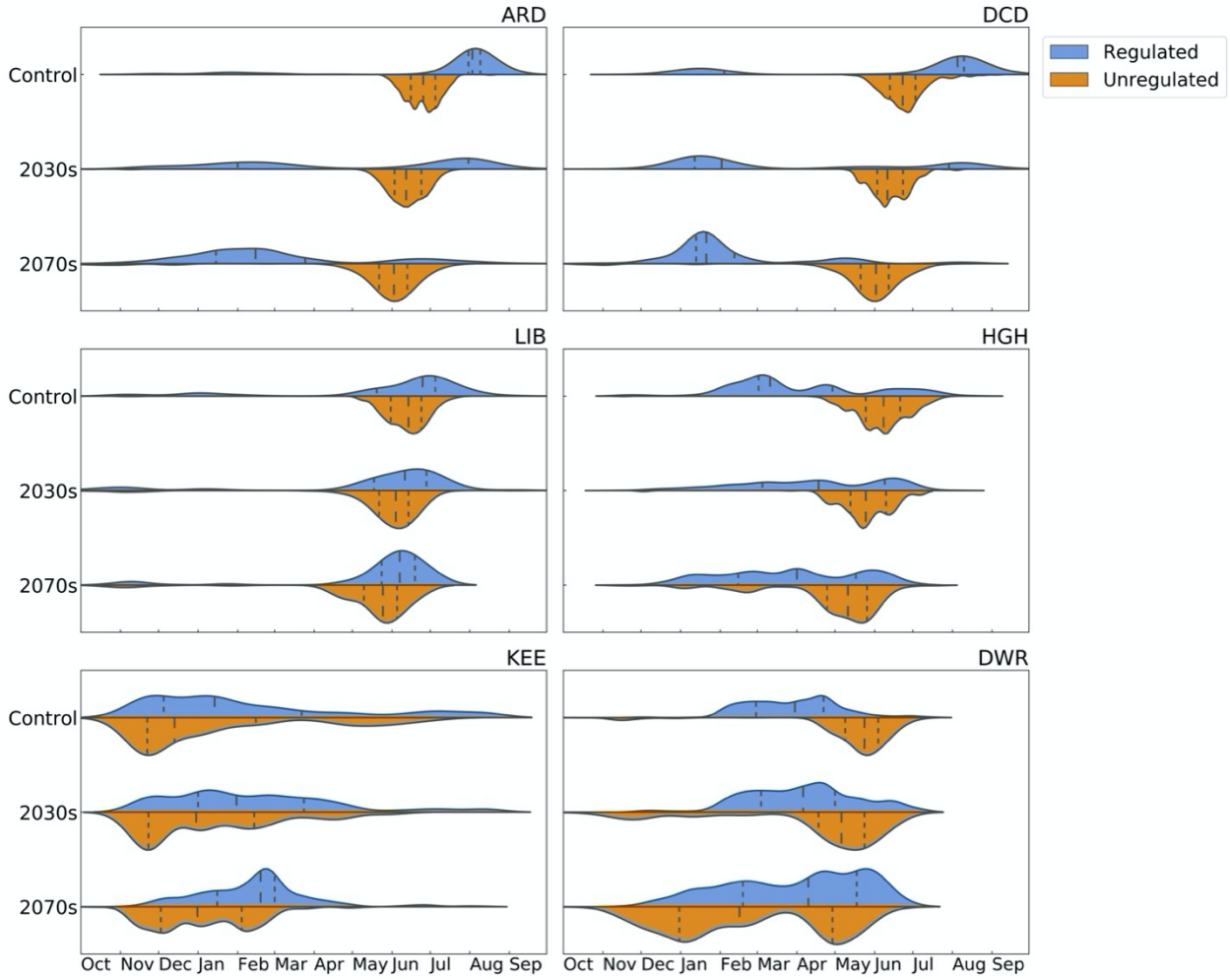

Figure A-6. Statistically smoothed distributions of the top 5 annual peak flow events for each 30-year period across the ensemble. Short, dashed lines indicate the 25th and 75th quantiles of the spread. Long, dashed lines indicate the median. Regulated peak flows are projected to increase in the winter at Arrow Lakes (ARD) and Duncan (DCD). Hungry Horse (HGH), Libby (LIB), Dworshak (DWR) peak flows are projected to increase in the spring. Yakima (KEE) shows large shifts in late winter peak flows. Figure adapted from Queen et al. (2021).

A.4 Seasonal Volume Percent Change and Uncertainty

Table A-1. September-October (SON) Volume Percent Change. U is unregulated, R is regulated. Table shows the (10^{th}) 50^{th} (90^{th}) percentiles of the ensemble. For each region, locations are sorted from upstream (top) to downstream (bottom) based on position of tributary confluence with the next lowest order stream using a top-down stream order approach (e.g., a headwater tributary has a higher stream order than the mainstem).

SON

Region	Site ID	2030 U	2030 R	2070 U	2070 R
Upper Columbia	MCD	(-18) -11 (0)	(-5) 5 (15)	(-29) -14 (13)	(3) 20 (30)
	RVC	(-16) -9 (1)	(-6) 4 (12)	(-22) -8 (18)	(4) 17 (29)
	ARD	(-16) -7 (4)	(-11) -6 (-2)	(-20) -5 (20)	(-22) -11 (-4)
	MUC	(-17) -8 (5)	(-13) -8 (-2)	(-20) -8 (17)	(-23) -12 (-4)
Kootenai	LIB	(-21) -10 (6)	(-19) -11 (-2)	(-28) -12 (11)	(-31) -18 (-4)
	BFE	(-19) -8 (8)	(-16) -10 (0)	(-25) -12 (14)	(-30) -15 (0)
	DCD	(-19) -7 (13)	(-16) -9 (0)	(-32) 2 (34)	(-24) -13 (8)
	CAN	(-17) -8 (7)	(-17) -12 (0)	(-25) -12 (17)	(-28) -14 (2)
	BRI	(-18) -8 (8)	(-17) -11 (0)	(-24) -11 (17)	(-27) -15 (3)
Pend Oreille	HGH	(-27) -8 (14)	(-7) -1 (5)	(-39) -19 (20)	(-10) -1 (5)
	CFM	(-25) -5 (17)	(-10) -3 (8)	(-30) -13 (24)	(-14) -5 (13)
	KER	(-23) -6 (11)	(-14) -8 (0)	(-32) -15 (20)	(-36) -17 (-6)
	TOM	(-16) -3 (10)	(-13) -5 (2)	(-25) -9 (19)	(-29) -12 (1)
	NOX	(-17) -5 (9)	(-13) -6 (1)	(-26) -11 (16)	(-30) -13 (0)
	CAB	(-17) -4 (9)	(-14) -6 (2)	(-26) -10 (16)	(-30) -12 (0)
	PSL	(-17) -2 (20)	(-10) -4 (6)	(-15) 10 (43)	(-12) -1 (12)
	ALF	(-15) -3 (10)	(-9) -4 (1)	(-23) -8 (17)	(-20) -9 (0)
	BOX	(-15) -3 (10)	(-9) -4 (1)	(-23) -8 (17)	(-21) -9 (0)
	BDY	(-15) -3 (10)	(-9) -4 (1)	(-23) -8 (16)	(-21) -9 (0)
	SEV	(-15) -3 (10)	(-10) -4 (1)	(-23) -7 (16)	(-21) -9 (0)
Spokane	PFL	(-20) -2 (31)	(-13) -3 (12)	(-19) 2 (55)	(-15) -4 (19)
	MON	(-19) -3 (24)	(-13) -4 (11)	(-18) -1 (42)	(-15) -5 (15)
	NIN	(-18) -2 (24)	(-13) -3 (10)	(-17) 0 (35)	(-14) -4 (14)
	LFL	(-17) -2 (22)	(-13) -3 (10)	(-15) 1 (29)	(-14) -3 (12)
Middle Columbia	GCL	(-15) -5 (8)	(-11) -7 (0)	(-19) -6 (19)	(-21) -12 (-2)
	CHL	(-16) -3 (14)	(-12) -4 (8)	(-19) 5 (44)	(-21) -6 (20)
	CHJ	(-15) -5 (8)	(-11) -7 (0)	(-19) -7 (19)	(-21) -12 (-2)
	WEL	(-15) -4 (9)	(-11) -7 (0)	(-18) -5 (19)	(-20) -11 (-1)
	RRH	(-15) -5 (9)	(-11) -7 (0)	(-18) -5 (19)	(-20) -11 (0)

	RIS	(-15) -4 (9)	(-11) -6 (0)	(-17) -4 (19)	(-19) -10 (0)
	WAN	(-15) -4 (9)	(-11) -7 (0)	(-17) -4 (19)	(-20) -10 (0)
	PRD	(-15) -5 (9)	(-11) -7 (0)	(-17) -4 (19)	(-20) -10 (0)
Yakima	KEE	(-29) 0 (19)	(-31) -20 (-6)	(-39) 10 (34)	(-42) -30 (-20)
	KAC	(-26) 0 (25)	(-8) 0 (6)	(-39) 13 (39)	(-30) -12 (4)
	CLE	(-23) -2 (18)	(-39) -27 (-17)	(-34) 8 (35)	(-49) -38 (-25)
	BUM	(-18) -2 (21)	(-19) -6 (11)	(-20) 2 (49)	(-25) -4 (22)
	RIM	(-18) -3 (14)	(-5) -1 (5)	(-24) -4 (29)	(-21) -9 (1)
Upper Snake	JCKY	(-8) 0 (9)	(-5) 0 (3)	(-13) 1 (30)	(-19) -8 (2)
	PALI	(-5) 0 (13)	(-13) -7 (4)	(-7) 6 (28)	(-26) -12 (8)
	HEII	(-5) 0 (12)	(-12) -6 (5)	(-7) 6 (26)	(-24) -10 (9)
	LORI	(-5) 0 (12)	(-13) -5 (12)	(-7) 6 (26)	(-24) -7 (21)
	REXI	(-5) 0 (12)	(-3) 2 (10)	(-13) 0 (20)	(-6) 3 (16)
	SHYI	(-7) -1 (10)	(-11) -3 (10)	(-15) 0 (18)	(-23) -9 (13)
	BFTI	(-7) -1 (11)	(-12) -2 (13)	(-15) 0 (19)	(-26) -9 (17)
	AMFI	(-6) 0 (11)	(-15) -8 (1)	(-11) 2 (26)	(-31) -19 (-3)
	MILI	(-5) 0 (10)	(-36) -14 (14)	(-11) 2 (30)	(-56) -35 (14)
	KIMI	(-5) 0 (11)	(-27) -10 (13)	(-10) 3 (31)	(-42) -24 (15)
	SKHI	(-2) 3 (13)	(-4) 3 (11)	(-1) 8 (42)	(-1) 5 (30)
	SWAI	(-1) 5 (16)	(-2) 6 (14)	(0) 10 (44)	(0) 10 (37)
	ANDI	(-2) 11 (31)	(-9) 1 (9)	(5) 25 (60)	(-18) 0 (14)
	ARKI	(-2) 10 (29)	(-13) 2 (23)	(2) 20 (52)	(-19) 4 (33)
	LUCI	(-2) 9 (28)	(-14) -1 (9)	(1) 18 (52)	(-22) -3 (13)
	BIGI	(-2) 7 (24)	(-18) -1 (27)	(-2) 14 (46)	(-12) 12 (62)
	OWY	(0) 27 (65)	(-6) 2 (14)	(-2) 48 (143)	(-8) 5 (94)
	SNYI	(-1) 8 (20)	(-4) 4 (15)	(1) 14 (47)	(-1) 11 (39)
	DEDI	(-16) -4 (30)	(-15) 6 (30)	(-30) 1 (59)	(-14) 13 (38)
	PABI	(-13) 1 (26)	(-14) -4 (7)	(-27) 9 (54)	(-24) -13 (3)
	HRSI	(-10) 4 (27)	(-7) 1 (19)	(-17) 10 (47)	(-12) 4 (29)
	PRPI	(-16) 1 (23)	(-26) -12 (13)	(-29) 6 (43)	(-38) -15 (24)
	WEII	(-2) 8 (22)	(-5) 3 (14)	(1) 15 (44)	(-3) 9 (35)
	BRN	(-2) 7 (23)	(-5) 3 (14)	(1) 15 (43)	(-2) 9 (35)
	OXB	(-2) 7 (22)	(-5) 3 (14)	(1) 15 (43)	(-2) 9 (35)
Lower Snake	ANA	(-5) 4 (17)	(-6) 2 (15)	(-2) 9 (37)	(-4) 6 (31)
	DWR	(-15) -5 (17)	(-16) -8 (-2)	(-20) -4 (27)	(-26) -12 (-1)
	SPD	(-17) -4 (20)	(-16) -7 (6)	(-22) -4 (30)	(-21) -10 (11)
	LWG	(-7) 3 (16)	(-7) 0 (12)	(-5) 6 (34)	(-7) 2 (25)
	LGS	(-7) 3 (16)	(-7) 0 (12)	(-5) 6 (33)	(-7) 2 (25)
	LMN	(-8) 2 (16)	(-8) 0 (12)	(-6) 5 (32)	(-9) 0 (22)
	IHR	(-8) 2 (16)	(-8) 0 (12)	(-6) 5 (31)	(-9) 0 (22)

	MCN	(-10) -2 (9)	(-10) -5 (2)	(-14) 0 (20)	(-17) -9 (4)
Lower Columbia	JDA	(-11) -2 (9)	(-10) -5 (1)	(-14) 0 (20)	(-17) -9 (4)
	TDA	(-10) -2 (9)	(-10) -5 (2)	(-13) 0 (20)	(-17) -9 (4)
	BON	(-10) -2 (8)	(-10) -5 (1)	(-13) -1 (19)	(-17) -9 (3)
Willamette	SVN	(-15) -2 (10)	(-16) -3 (8)	(-27) -4 (10)	(-27) -6 (8)

Table A-2. December-February (DJF) Volume Percent Change. U is unregulated, R is regulated. Table shows the (10^{th}) 50^{th} (90^{th}) percentiles of the ensemble. For each region, locations are sorted from upstream (top) to downstream (bottom) based on position of tributary confluence with the next lowest order stream using a top-down stream order approach (e.g., a headwater tributary has a higher stream order than the mainstem).

DJF

Region	Site ID	2030 U	2030 R	2070 U	2070 R
Upper Columbia	MCD	(-3) 17 (41)	(-12) -8 (0)	(10) 56 (106)	(-33) -18 (-7)
	RVC	(-2) 21 (44)	(-10) -6 (2)	(12) 65 (116)	(-27) -12 (0)
	ARD	(0) 24 (49)	(-8) -1 (2)	(16) 73 (120)	(-25) -5 (4)
	MUC	(3) 22 (48)	(-8) 0 (7)	(35) 66 (120)	(-13) 0 (13)
Kootenai	LIB	(-4) 14 (36)	(-17) -2 (10)	(14) 56 (105)	(-21) -2 (14)
	BFE	(0) 22 (51)	(-14) 2 (13)	(39) 66 (134)	(-9) 10 (32)
	DCD	(-2) 24 (51)	(-7) 1 (9)	(10) 80 (127)	(-22) 0 (15)
	CAN	(1) 23 (51)	(-10) 5 (15)	(44) 66 (134)	(0) 8 (38)
	BRI	(1) 22 (50)	(-10) 5 (16)	(43) 65 (133)	(2) 10 (40)
Pend Oreille	HGH	(-1) 40 (86)	(-24) -12 (6)	(44) 140 (266)	(-40) -23 (9)
	CFM	(4) 40 (82)	(-8) 5 (23)	(48) 137 (246)	(1) 26 (76)
	KER	(5) 40 (80)	(-4) 4 (16)	(51) 133 (235)	(0) 16 (49)
	TOM	(4) 34 (68)	(-2) 11 (25)	(59) 100 (184)	(16) 29 (74)
	NOX	(5) 38 (77)	(-1) 12 (29)	(68) 114 (211)	(19) 32 (80)
	CAB	(4) 36 (75)	(-1) 14 (31)	(66) 108 (202)	(21) 34 (84)
	PSL	(9) 58 (101)	(4) 50 (91)	(78) 178 (281)	(53) 137 (230)
	ALF	(6) 36 (71)	(0) 17 (35)	(63) 103 (194)	(24) 38 (82)
	BOX	(6) 35 (70)	(0) 17 (35)	(62) 102 (192)	(24) 39 (82)
	BDY	(6) 35 (70)	(0) 17 (35)	(61) 100 (191)	(24) 39 (83)
	SEV	(5) 34 (71)	(-1) 17 (36)	(60) 100 (192)	(25) 41 (85)
Spokane	PFL	(24) 69 (108)	(22) 61 (105)	(114) 178 (223)	(106) 167 (205)
	MON	(18) 60 (98)	(17) 53 (92)	(104) 158 (190)	(93) 147 (177)
	NIN	(15) 55 (92)	(15) 49 (87)	(97) 148 (172)	(86) 136 (162)
	LFL	(14) 51 (88)	(14) 45 (81)	(90) 139 (162)	(78) 122 (146)
Middle Columbia	GCL	(6) 30 (55)	(-6) 6 (15)	(55) 84 (143)	(3) 12 (32)

	CHL	(-5) 34 (75)	(-1) 3 (10)	(13) 130 (210)	(0) 15 (28)
	CHJ	(6) 30 (54)	(-6) 6 (15)	(54) 83 (142)	(3) 12 (32)
	WEL	(5) 30 (54)	(-6) 6 (15)	(54) 85 (143)	(3) 13 (34)
	RRH	(5) 30 (55)	(-6) 6 (15)	(54) 85 (145)	(3) 13 (34)
	RIS	(5) 30 (57)	(-5) 7 (16)	(55) 89 (148)	(4) 14 (36)
	WAN	(5) 30 (57)	(-5) 7 (16)	(55) 89 (149)	(4) 14 (37)
	PRD	(5) 30 (57)	(-5) 7 (16)	(55) 90 (149)	(4) 14 (37)
Yakima	KEE	(19) 52 (85)	(-18) 1 (31)	(90) 131 (174)	(-16) 21 (63)
	KAC	(16) 52 (84)	(-19) -3 (12)	(89) 135 (184)	(-18) 4 (74)
	CLE	(2) 51 (91)	(-30) -10 (17)	(60) 179 (289)	(-32) 6 (51)
	BUM	(15) 58 (107)	(8) 28 (70)	(95) 186 (273)	(52) 104 (184)
	RIM	(7) 34 (78)	(-27) -10 (72)	(64) 110 (185)	(-21) 29 (253)
Upper Snake	JCKY	(-3) 9 (29)	(-6) -1 (7)	(7) 57 (149)	(-6) 5 (33)
	PALI	(2) 16 (38)	(-9) 7 (27)	(24) 65 (142)	(7) 37 (94)
	HEII	(3) 16 (37)	(-7) 9 (28)	(25) 63 (133)	(10) 38 (92)
	LORI	(3) 16 (37)	(-7) 10 (28)	(26) 63 (133)	(10) 39 (94)
	REXI	(4) 22 (39)	(0) 13 (25)	(26) 72 (135)	(14) 42 (82)
	SHYI	(5) 22 (43)	(-4) 13 (30)	(32) 82 (172)	(15) 47 (106)
	BFTI	(5) 23 (44)	(-3) 13 (30)	(35) 88 (184)	(15) 47 (107)
	AMFI	(6) 23 (43)	(-18) 4 (36)	(36) 82 (164)	(-11) 35 (116)
	MILI	(8) 28 (46)	(-16) 6 (35)	(40) 85 (162)	(-4) 43 (118)
	KIMI	(8) 27 (45)	(-15) 7 (35)	(39) 82 (154)	(-2) 43 (113)
	SKHI	(6) 25 (38)	(-6) 11 (26)	(33) 70 (131)	(3) 37 (93)
	SWAI	(6) 24 (41)	(-4) 14 (31)	(31) 68 (122)	(6) 40 (95)
	ANDI	(10) 48 (105)	(-12) 10 (51)	(50) 178 (365)	(10) 63 (176)
	ARKI	(21) 57 (110)	(-12) 11 (53)	(84) 190 (331)	(19) 91 (226)
	LUCI	(21) 60 (112)	(-16) 22 (81)	(91) 192 (321)	(37) 130 (281)
	BIGI	(22) 61 (116)	(-9) 29 (101)	(95) 193 (323)	(54) 153 (321)
	OWY	(27) 79 (150)	(53) 309 (1567)	(81) 212 (395)	(227) 997 (5000)
	SNYI	(10) 32 (50)	(-3) 21 (44)	(44) 87 (158)	(17) 61 (131)
	DEDI	(1) 51 (114)	(-6) 3 (33)	(69) 204 (401)	(6) 50 (232)
	PABI	(24) 90 (154)	(-6) 23 (89)	(152) 281 (447)	(30) 109 (221)
	HRSI	(15) 61 (110)	(2) 31 (78)	(105) 201 (318)	(46) 116 (218)
	PRPI	(23) 69 (112)	(-17) 15 (57)	(140) 204 (311)	(17) 83 (164)
	WEII	(14) 39 (57)	(-1) 21 (41)	(59) 104 (176)	(28) 70 (141)
	BRN	(14) 39 (59)	(-3) 23 (43)	(61) 107 (176)	(30) 71 (139)
	OXB	(14) 39 (59)	(-3) 23 (43)	(61) 107 (176)	(30) 71 (139)
Lower Snake	ANA	(12) 34 (60)	(0) 25 (46)	(57) 103 (171)	(35) 74 (143)
	DWR	(20) 64 (97)	(-10) 15 (44)	(121) 187 (260)	(18) 44 (80)
	SPD	(18) 61 (104)	(0) 37 (73)	(111) 169 (256)	(58) 92 (160)

	LWG	(8) 36 (63)	(-2) 22 (48)	(67) 106 (168)	(39) 74 (134)
	LGS	(8) 36 (63)	(-2) 22 (48)	(67) 106 (168)	(39) 74 (134)
	LMN	(9) 39 (67)	(-2) 24 (51)	(72) 113 (176)	(42) 79 (141)
	IHR	(9) 39 (67)	(-2) 24 (51)	(71) 113 (176)	(42) 79 (141)
	MCN	(9) 31 (57)	(-2) 11 (23)	(59) 95 (152)	(12) 29 (57)
Lower Columbia	JDA	(8) 32 (56)	(-1) 11 (24)	(60) 95 (150)	(14) 31 (58)
	TDA	(8) 31 (56)	(-1) 12 (25)	(59) 92 (146)	(14) 31 (58)
	BON	(8) 32 (56)	(-1) 13 (26)	(61) 91 (142)	(15) 32 (59)
Willamette	SVN	(2) 16 (27)	(2) 17 (28)	(22) 28 (40)	(23) 29 (41)

Table A-3. March-May (MAM) Volume Percent Change. U is unregulated, R is regulated. Table shows the (10^{th}) 50^{th} (90^{th}) percentiles of the ensemble. For each region, locations are sorted from upstream (top) to downstream (bottom) based on position of tributary confluence with the next lowest order stream using a top-down stream order approach (e.g., a headwater tributary has a higher stream order than the mainstem).

MAM

Region	Site ID	2030 U	2030 R	2070 U	2070 R
Upper Columbia	MCD	(18) 33 (57)	(0) 17 (42)	(59) 95 (151)	(17) 63 (110)
	RVC	(19) 30 (56)	(10) 23 (43)	(58) 92 (142)	(42) 70 (114)
	ARD	(16) 28 (50)	(2) 21 (46)	(49) 78 (119)	(34) 55 (95)
	MUC	(9) 26 (43)	(3) 22 (39)	(43) 65 (96)	(38) 52 (88)
Kootenai	LIB	(7) 29 (46)	(1) 23 (38)	(42) 67 (106)	(33) 49 (75)
	BFE	(5) 25 (38)	(1) 21 (33)	(35) 54 (80)	(28) 42 (65)
	DCD	(13) 35 (58)	(9) 41 (79)	(51) 89 (145)	(77) 140 (214)
	CAN	(6) 27 (40)	(4) 25 (42)	(36) 60 (87)	(39) 58 (91)
	BRI	(6) 27 (41)	(4) 26 (42)	(36) 60 (88)	(39) 58 (93)
Pend Oreille	HGH	(17) 38 (61)	(0) 10 (23)	(49) 79 (118)	(8) 25 (56)
	CFM	(14) 34 (54)	(8) 24 (38)	(42) 70 (100)	(33) 50 (78)
	KER	(13) 33 (51)	(9) 27 (45)	(42) 67 (97)	(42) 60 (99)
	TOM	(12) 31 (44)	(8) 29 (41)	(39) 56 (80)	(38) 55 (84)
	NOX	(12) 30 (44)	(8) 29 (41)	(38) 56 (79)	(38) 55 (84)
	CAB	(11) 29 (43)	(8) 28 (40)	(36) 54 (75)	(36) 53 (81)
	PSL	(5) 17 (28)	(9) 27 (42)	(10) 28 (49)	(28) 50 (76)
	ALF	(9) 25 (38)	(8) 28 (42)	(29) 47 (68)	(38) 56 (87)
	BOX	(9) 25 (37)	(8) 28 (42)	(28) 46 (67)	(39) 56 (87)
	BDY	(9) 25 (37)	(8) 28 (42)	(28) 46 (67)	(38) 57 (86)
	SEV	(8) 25 (37)	(8) 28 (42)	(27) 46 (67)	(37) 56 (86)
Spokane	PFL	(-8) 1 (11)	(-4) 5 (18)	(-23) -9 (17)	(-16) 0 (33)

	MON	(-7) 1 (10)	(-4) 6 (18)	(-21) -9 (17)	(-14) 2 (33)
	NIN	(-7) 1 (10)	(-4) 6 (18)	(-20) -7 (18)	(-13) 3 (33)
	LFL	(-7) 1 (10)	(-4) 6 (17)	(-19) -6 (19)	(-12) 3 (33)
Middle Columbia	GCL	(7) 23 (35)	(3) 21 (29)	(33) 50 (73)	(27) 41 (65)
	CHL	(9) 32 (61)	(12) 55 (93)	(49) 77 (147)	(98) 152 (241)
	CHJ	(7) 23 (35)	(3) 21 (29)	(33) 50 (74)	(27) 41 (65)
	WEL	(7) 24 (35)	(2) 22 (29)	(33) 50 (74)	(30) 42 (64)
	RRH	(7) 25 (35)	(2) 23 (29)	(35) 52 (75)	(32) 44 (65)
	RIS	(7) 24 (35)	(2) 23 (29)	(35) 52 (74)	(32) 45 (64)
	WAN	(7) 25 (35)	(2) 23 (29)	(35) 52 (75)	(33) 45 (65)
	PRD	(7) 25 (35)	(2) 23 (29)	(35) 52 (75)	(33) 46 (65)
Yakima	KEE	(-2) 8 (18)	(-14) 0 (16)	(-24) -5 (17)	(-20) 8 (26)
	KAC	(-2) 7 (17)	(-39) -11 (14)	(-28) -5 (19)	(-37) -2 (25)
	CLE	(18) 36 (60)	(-11) 4 (25)	(37) 61 (110)	(18) 43 (99)
	BUM	(10) 27 (49)	(13) 37 (70)	(7) 30 (59)	(26) 60 (85)
	RIM	(0) 13 (29)	(-18) 0 (31)	(-10) 16 (41)	(-9) 16 (52)
Upper Snake	JCKY	(17) 44 (78)	(15) 57 (119)	(71) 93 (164)	(107) 161 (312)
	PALI	(14) 32 (61)	(9) 28 (58)	(45) 75 (134)	(44) 69 (128)
	HEII	(13) 30 (59)	(9) 27 (56)	(42) 72 (129)	(42) 66 (123)
	LORI	(13) 30 (59)	(10) 32 (69)	(42) 72 (129)	(50) 82 (148)
	REXI	(11) 27 (56)	(14) 35 (69)	(37) 60 (109)	(43) 74 (136)
	SHYI	(14) 31 (60)	(13) 36 (75)	(48) 72 (129)	(59) 90 (164)
	BFTI	(14) 31 (62)	(16) 42 (85)	(49) 73 (132)	(66) 102 (188)
	AMFI	(12) 30 (61)	(19) 33 (63)	(45) 71 (122)	(57) 82 (159)
	MILI	(13) 30 (59)	(30) 66 (117)	(43) 73 (118)	(97) 162 (264)
	KIMI	(13) 29 (58)	(29) 63 (110)	(42) 72 (116)	(91) 154 (248)
	SKHI	(14) 26 (49)	(15) 36 (65)	(35) 64 (101)	(51) 89 (144)
	SWAI	(13) 27 (49)	(16) 37 (67)	(33) 62 (96)	(50) 89 (140)
	ANDI	(10) 30 (70)	(21) 49 (81)	(28) 54 (147)	(60) 98 (169)
	ARKI	(9) 26 (46)	(19) 42 (63)	(22) 45 (93)	(48) 74 (125)
	LUCI	(9) 25 (47)	(19) 42 (66)	(18) 44 (88)	(48) 76 (136)
	BIGI	(10) 24 (46)	(23) 57 (96)	(18) 43 (85)	(66) 107 (204)
	OWY	(-8) 21 (65)	(-3) 55 (137)	(0) 40 (153)	(27) 87 (259)
	SNYI	(12) 28 (47)	(20) 45 (74)	(30) 63 (92)	(55) 99 (172)
	DEDI	(26) 45 (133)	(-1) 59 (141)	(43) 73 (356)	(92) 170 (317)
	PABI	(7) 21 (36)	(11) 30 (52)	(3) 28 (64)	(25) 54 (91)
	HRSI	(12) 25 (56)	(7) 20 (50)	(13) 34 (110)	(11) 35 (118)
	PRPI	(9) 24 (52)	(1) 17 (54)	(14) 32 (97)	(6) 32 (124)
	WEII	(10) 25 (43)	(12) 34 (58)	(25) 54 (84)	(36) 74 (134)
	BRN	(10) 25 (42)	(12) 32 (59)	(24) 52 (81)	(35) 72 (135)

	OXB	(10) 24 (42)	(12) 32 (59)	(24) 51 (81)	(35) 72 (135)
Lower Snake	ANA	(15) 25 (41)	(18) 30 (49)	(28) 50 (82)	(38) 63 (103)
	DWR	(4) 14 (26)	(-2) 7 (19)	(-1) 11 (42)	(5) 16 (34)
	SPD	(5) 17 (30)	(3) 17 (26)	(5) 18 (47)	(9) 23 (43)
	LWG	(12) 22 (36)	(14) 25 (40)	(24) 44 (67)	(31) 53 (81)
	LGS	(13) 22 (36)	(15) 25 (40)	(24) 45 (68)	(32) 53 (82)
	LMN	(13) 23 (36)	(15) 26 (41)	(24) 45 (68)	(32) 54 (83)
	IHR	(13) 23 (37)	(15) 26 (41)	(24) 45 (69)	(32) 54 (83)
	MCN	(7) 24 (34)	(4) 25 (33)	(33) 48 (69)	(37) 47 (68)
Lower Columbia	JDA	(7) 25 (33)	(4) 25 (33)	(33) 48 (68)	(38) 47 (68)
	TDA	(7) 24 (33)	(4) 25 (32)	(33) 46 (67)	(37) 45 (66)
	BON	(7) 23 (32)	(4) 24 (31)	(32) 44 (64)	(34) 43 (63)
Willamette	SVN	(-15) -5 (0)	(-14) -4 (0)	(-22) -11 (1)	(-21) -10 (2)

Table A-4. June-August (JJA) Volume Percent Change. U is unregulated, R is regulated. Table shows the (10^{th}) 50^{th} (90^{th}) percentiles of the ensemble. For each region, locations are sorted from upstream (top) to downstream (bottom) based on position of tributary confluence with the next lowest order stream using a top-down stream order approach (e.g., a headwater tributary has a higher stream order than the mainstem).

JJA

Region	Site ID	2030 U	2030 R	2070 U	2070 R
Upper Columbia	MCD	(-9) -5 (-1)	(-2) 14 (25)	(-33) -20 (-6)	(3) 21 (39)
	RVC	(-10) -6 (-2)	(-8) 1 (8)	(-36) -23 (-8)	(-15) -4 (6)
	ARD	(-12) -8 (-4)	(-2) 4 (13)	(-39) -26 (-12)	(0) 12 (21)
	MUC	(-17) -12 (-8)	(-9) -5 (1)	(-45) -31 (-17)	(-17) -10 (-2)
Kootenai	LIB	(-22) -14 (-10)	(-14) -5 (2)	(-51) -37 (-20)	(-20) -9 (-1)
	BFE	(-23) -17 (-11)	(-19) -11 (-2)	(-52) -39 (-22)	(-31) -19 (-13)
	DCD	(-10) -6 (-1)	(-4) 3 (21)	(-38) -24 (-9)	(-30) -11 (16)
	CAN	(-22) -16 (-10)	(-18) -11 (-5)	(-53) -39 (-21)	(-39) -28 (-15)
	BRI	(-23) -16 (-11)	(-19) -12 (-7)	(-54) -40 (-22)	(-42) -30 (-17)
Pend Oreille	HGH	(-34) -22 (-13)	(-15) 1 (24)	(-65) -54 (-31)	(-12) 0 (17)
	CFM	(-31) -23 (-14)	(-26) -16 (-11)	(-63) -53 (-31)	(-51) -39 (-24)
	KER	(-31) -22 (-13)	(-25) -16 (-8)	(-62) -51 (-30)	(-48) -38 (-23)
	TOM	(-29) -20 (-13)	(-27) -17 (-10)	(-60) -45 (-28)	(-54) -41 (-26)
	NOX	(-30) -21 (-13)	(-29) -18 (-11)	(-61) -47 (-29)	(-56) -43 (-27)
	CAB	(-30) -21 (-13)	(-28) -18 (-11)	(-60) -46 (-29)	(-55) -42 (-27)
	PSL	(-40) -30 (-17)	(-40) -29 (-15)	(-67) -54 (-38)	(-69) -56 (-34)
	ALF	(-30) -21 (-13)	(-29) -19 (-11)	(-58) -45 (-28)	(-56) -43 (-27)

	BOX	(-29) -21 (-13)	(-28) -19 (-10)	(-58) -44 (-28)	(-55) -42 (-26)
	BDY	(-29) -21 (-13)	(-28) -19 (-10)	(-58) -44 (-28)	(-55) -42 (-26)
	SEV	(-29) -21 (-13)	(-28) -19 (-10)	(-58) -45 (-28)	(-55) -42 (-26)
Spokane	PFL	(-49) -38 (-21)	(-52) -41 (-23)	(-72) -61 (-49)	(-75) -65 (-54)
	MON	(-44) -34 (-19)	(-49) -38 (-22)	(-67) -55 (-44)	(-73) -62 (-50)
	NIN	(-42) -32 (-18)	(-46) -36 (-21)	(-63) -52 (-40)	(-70) -58 (-46)
	LFL	(-40) -30 (-17)	(-44) -33 (-20)	(-61) -50 (-38)	(-67) -55 (-43)
Middle Columbia	GCL	(-20) -14 (-10)	(-15) -9 (-3)	(-48) -36 (-22)	(-27) -18 (-11)
	CHL	(-31) -14 (-4)	(-49) -19 (-1)	(-63) -40 (-15)	(-88) -64 (-19)
	CHJ	(-20) -14 (-9)	(-14) -9 (-3)	(-48) -36 (-22)	(-27) -18 (-11)
	WEL	(-21) -14 (-10)	(-15) -10 (-4)	(-49) -37 (-22)	(-29) -19 (-14)
	RRH	(-21) -14 (-10)	(-16) -10 (-4)	(-49) -37 (-22)	(-31) -20 (-15)
	RIS	(-21) -15 (-10)	(-17) -10 (-5)	(-50) -37 (-22)	(-32) -21 (-16)
	WAN	(-21) -14 (-10)	(-17) -10 (-5)	(-50) -37 (-22)	(-32) -21 (-15)
	PRD	(-21) -14 (-10)	(-17) -10 (-5)	(-50) -37 (-22)	(-32) -21 (-16)
Yakima	KEE	(-63) -42 (-24)	(0) 6 (16)	(-81) -68 (-43)	(-2) 12 (28)
	KAC	(-62) -41 (-25)	(-1) 10 (35)	(-80) -69 (-46)	(5) 37 (80)
	CLE	(-41) -24 (-11)	(3) 6 (12)	(-80) -59 (-29)	(-4) 7 (13)
	BUM	(-53) -34 (-20)	(-41) -25 (-13)	(-81) -64 (-39)	(-67) -51 (-27)
	RIM	(-37) -25 (-14)	(-4) 1 (6)	(-64) -47 (-27)	(-8) 1 (8)
Upper Snake	JCKY	(-27) -14 (-1)	(-12) -5 (4)	(-56) -43 (-17)	(-31) -18 (-3)
	PALI	(-25) -13 (0)	(-11) -3 (5)	(-49) -37 (-14)	(-26) -16 (-2)
	HEII	(-24) -12 (0)	(-11) -3 (5)	(-47) -36 (-14)	(-26) -16 (-2)
	LORI	(-24) -12 (0)	(-16) -4 (10)	(-47) -36 (-14)	(-38) -24 (-3)
	REXI	(-17) -9 (0)	(-18) -9 (1)	(-40) -29 (-9)	(-40) -29 (-9)
	SHYI	(-22) -11 (0)	(-19) -6 (8)	(-45) -34 (-12)	(-47) -33 (-7)
	BFTI	(-22) -11 (0)	(-27) -7 (11)	(-46) -35 (-12)	(-63) -45 (-8)
	AMFI	(-21) -10 (1)	(-2) 4 (11)	(-43) -32 (-10)	(-13) -7 (9)
	MILI	(-20) -10 (1)	(-24) 8 (52)	(-44) -32 (-10)	(-79) -47 (31)
	KIMI	(-19) -10 (1)	(-20) 8 (46)	(-43) -31 (-10)	(-69) -40 (29)
	SKHI	(-15) -7 (4)	(-5) 9 (25)	(-36) -23 (-4)	(-16) -1 (29)
	SWAI	(-14) -5 (6)	(-7) 8 (23)	(-33) -18 (0)	(-20) -1 (32)
	ANDI	(-27) -12 (3)	(-17) -7 (6)	(-53) -35 (-8)	(-30) -19 (1)
	ARKI	(-27) -12 (0)	(-15) -7 (3)	(-52) -35 (-8)	(-33) -19 (-1)
	LUCI	(-27) -12 (0)	(-13) -5 (3)	(-52) -36 (-10)	(-29) -16 (0)
	BIGI	(-27) -11 (0)	(-20) -9 (12)	(-51) -34 (-8)	(-42) -24 (10)
	OWY	(-24) 6 (58)	(-11) 0 (23)	(-30) 4 (110)	(-18) -1 (37)
	SNYI	(-15) -5 (6)	(-10) 5 (24)	(-33) -16 (2)	(-24) -2 (29)
	DEDI	(-39) -20 (-6)	(-10) -1 (10)	(-65) -54 (-29)	(-21) -11 (2)
	PABI	(-40) -23 (-10)	(-18) -6 (1)	(-69) -53 (-30)	(-34) -23 (-3)

	HRSI	(-32) -18 (-7)	(-22) -12 (-3)	(-61) -47 (-26)	(-41) -29 (-13)
	PRPI	(-34) -18 (-7)	(-34) -16 (-4)	(-61) -47 (-25)	(-58) -42 (-16)
	WEII	(-16) -6 (3)	(-16) -1 (12)	(-36) -19 (-1)	(-32) -12 (14)
	BRN	(-17) -6 (3)	(-15) -1 (11)	(-36) -19 (-1)	(-30) -12 (14)
	OXB	(-17) -6 (3)	(-15) -1 (11)	(-36) -19 (-1)	(-30) -12 (14)
Lower Snake	ANA	(-22) -10 (-2)	(-24) -9 (-1)	(-45) -30 (-10)	(-48) -30 (-7)
	DWR	(-41) -29 (-18)	(-6) -1 (4)	(-67) -56 (-42)	(-15) -7 (-1)
	SPD	(-41) -25 (-18)	(-27) -16 (-10)	(-69) -55 (-40)	(-48) -36 (-26)
	LWG	(-26) -13 (-6)	(-24) -9 (-4)	(-48) -34 (-15)	(-45) -29 (-11)
	LGS	(-26) -13 (-6)	(-24) -9 (-3)	(-48) -34 (-15)	(-45) -29 (-11)
	LMN	(-28) -13 (-7)	(-26) -11 (-4)	(-50) -36 (-16)	(-48) -32 (-13)
	IHR	(-28) -13 (-7)	(-27) -11 (-4)	(-50) -36 (-16)	(-48) -32 (-13)
	MCN	(-21) -14 (-11)	(-17) -10 (-6)	(-49) -34 (-21)	(-36) -24 (-15)
Lower Columbia	JDA	(-21) -14 (-11)	(-17) -10 (-6)	(-49) -34 (-21)	(-36) -23 (-15)
	TDA	(-21) -14 (-11)	(-17) -10 (-6)	(-49) -34 (-21)	(-36) -23 (-15)
	BON	(-21) -14 (-11)	(-17) -10 (-6)	(-49) -34 (-21)	(-35) -23 (-15)
Willamette	SVN	(-38) -25 (-16)	(-35) -22 (-13)	(-58) -40 (-25)	(-54) -35 (-22)